

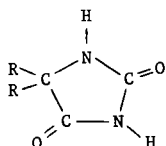
## THE MECHANISM OF THE FORMATION OF HYDANTOINS

J.J. Worman, K. Uhrich, E. Olson, J. Diehl  
S. Farnum, and S. Hawthorne

University of North Dakota Energy Research Center  
Box 8213, University Station  
Grand Forks, North Dakota 58202

### Introduction

Hydantions, (1), are biologically active compounds which occur in nature and have been isolated from such sources as sugar beets and butterfly wings. Synthetic analogs have found widespread use as anticonvulsant drugs, bacteriocides, stabilizers in photographic film, and in the preparation of high temperature epoxy resins. Uses, preparation, and reactions of hydantions have been extensively studied and are reported elsewhere (1, 2).



(1)

Recently a number of hydantoin isomers have been detected and identified in coal gasification condensate water from the gasification of Indian Head (ND) lignite at the University of North Dakota Energy Research Center in a slagging fixed bed gasifier (3). The hydantions constitute a major portion of the organics in the condensate water and have recently been identified in water from other gasification processes (5). In general the concentrations of hydantions found in the condensate water from an ash gasifier are smaller than those found from the slagging process. There is also a relationship between the type of coal used and the amount of hydantions formed. Lignite coal reacting in a slagging gasifier gives the largest concentration of hydantions in the condensate water. The major isomer in the coal gasification condensate water is 5,5-dimethylhydantoin (DMH). It should be emphasized that DMH is formed from individual species (acetone, cyanide, ammonia, and carbonate) in the condensate water and does not form directly in the gasifier. Hydantions were shown to be either absent or present in low concentrations in water samples which were collected from side-stream samples in the UNDERC gasifier and quickly frozen. When this sidestream condensed water was heated in a constant temperature bath of 40°C, DMH concentrations increased in an approximately second order manner (6). The formation is believed to proceed by the Bucherer-Berg reaction, the same reaction used for commercial hydantoin synthesis (3).

The potential use of the slagger to produce economically useful synthetic fuel gas, both on the national and international scale, prompted an investigation into the kinetics and mechanisms of formation of DMH. It was impossible to obtain reliable and reproducible concentration data for acetone and cyanide in the raw gasifier condensate water due to reversible addition products (acetone cyanohydrin, etc), so a model system was chosen. Acetone cyanohydrin was reacted with excess ammonium carbonate at concentrations approaching those obtained in the condensate water. The experimental details and results have been recently reported (7). The rate of formation of DMH was first order in all of the reactants as expressed by Equation 1.

$$\text{Rate of formation of DMH} = [\text{Acetone}] [\text{HCN}] [\text{NH}_3] [\text{CO}_2] \quad 1)$$

This kinetic data is valuable in predicting the rate of formation of DMH in coal gasification condensate water, provided the model is applicable. The pH of the model solution and the condensate water remained constant at around 8.4, but the effects of small changes in pH on the rate are not fully known.

A mechanism consistent with the kinetic data and partially verified by others is shown in Scheme 1 (8, 9, 10). What remains to be studied is to obtain detailed evidence of the rate-determining step and to isolate intermediates VI, VII, and VIII. In this work we will show that the carbamate salt which results from the reaction of two moles of  $\alpha$ -aminoisobutyronitrile with carbon dioxide gives an N-substituted hydantoin rather than the expected DMH. This either precludes the salt as forming in the gasifier water since the N-substituted hydantoins has not been identified in gasifier condensate water, or the salt reacts rapidly by an alternate mechanism to give DMH.

### Experimental

$\alpha$ -Aminoisobutyronitrile (IV) - Ammonia gas was bubbled into 50 ml of acetone cyanohydrin (Aldrich) at 60°C for several hours. The product was distilled at 50-56° (20 mm) to give 90 percent yield. The structure was verified by IR, Mass Spec. and <sup>13</sup>C NMR. The product was stored under nitrogen and refrigerated to prevent slow reverse hydrolysis and discoloration.

2-Cyanopropyl-ammonium 2-Cyanopropyl-2-Amino Carbamate (X) - Dry ice was added slowly to a 25-ml neat sample of  $\alpha$ -aminoisobutyronitrile. This was continued until the entire system was solid, about one hour. Anhydrous ether was added and the mixture stirred and filtered. The resulting white solid reacts with dilute hydrochloric acid to give the starting aminonitrile hydrochloride salt and carbon dioxide. The carbamate had a m.p. of 210°C and gave peaks at m/e 212 and 168 via solid probe mass spectrometry. On hydrolysis, the compound gave acetone, ammonia, acetone cyanohydrin, and  $\alpha$ -aminoisobutyronitrile as indicated by GC/MS.

#### N-( $\alpha$ -Carbamylisopropyl)-N'- $\alpha$ -isobutyronitrile urea (XI)

- A) Carbon dioxide was bubbled through a neat sample of a  $\alpha$ -Aminoisobutyronitrile at room temperature. After one hour, the entire sample was solid. This solid was filtered and washed thoroughly with anhydrous ether to remove any unreacted starting material. All spectral properties and elemental analyses were consistent with the structure. The m.p. was identical to the structure proposed by Bucherer (8).
- B) Compound X was allowed to stand at room temperature for several days and after analysis proved to be identical to XI in all respects.

3-( $\alpha$ -Carbamylisopropyl)-5,5-dimethylhydantoin (XIII) - The N-substituted urea, XI, was allowed to stand at room temperature in water for 24 hours. The reaction was followed by ultraviolet spectroscopy and by gas chromatography which indicated the formation of an intermediate that disappeared slowly to give the final product. After evaporation of the water in a vacuum, the resulting white solid (50% yield) was identified as 3-( $\alpha$ -carbamylisopropyl)-5,5-dimethylhydantoin (XIII). The structure was verified by <sup>13</sup>C-NMR and single crystal x-ray analysis. The properties of the solid were identical in all respects to that of a sample prepared by an alternate synthesis (11). The high resolution mass spectrum gave the correct molecular formula and a molecular ion of m/e 213 and a base peak at m/e 169.

### Results and Discussion

In order to clarify further the mechanism of formation of DMH shown in Scheme 1, an attempt was made to isolate the carbamic acid salt of X. When solid dry ice was added to  $\alpha$ -aminoisobutyronitrile, a white solid was isolated which by IR, mass spectrometry, elemental analysis, and its reaction with water and hydrochloric acid was best represented by structure XI. Salts of carbamic acids of similar structure have been reported previously and are more or less stable, depending on their specific structure (12). The carbamate X slowly rearranged at room temperature to the disubstituted urea, XI, shown in Scheme 2. This urea was also prepared by bubbling carbon dioxide gas through  $\alpha$ -aminoisobutyronitrile at room temperature.

The compound was reported previously (8). Its structure was verified by spectroscopic techniques and elemental analysis.

What occurred next was unexpected. When the N, N'-disubstituted urea was placed in water at room temperature, changes began to take place. The ultraviolet absorption spectrum showed a gradual increase in an absorption at 257 nm. This peak began to disappear after twelve hours and after twenty-four hours was absent from the spectrum. GC analysis using a cool, on-column injection onto a 30 m OV-351 fused silica capillary column gave, as a major compound, the N-substituted hydantoin, XIII. The structure of XIII was proven by alternate synthesis, elemental and spectral analysis, and single crystal X-ray analysis. The carbamate salt in water gave similar results. Only trace amounts of DMH were observed by GC/MS.

The mechanism for the formation of the N-substituted hydantoin is shown in Scheme 2. Evidence for the structure of the bicyclic imino intermediate (XII) is based on several factors. The ultraviolet absorption spectrum is consistent with an  $n \rightarrow \pi^*$  transition of an imine chromophore occurring at 257 nm (13) and the GC/MS of the intermediate gave a peak at m/e 195. This represented a loss of ammonia from the starting N-substitute area, XI. The absence of a fragment peak at m/e 151 (m-44) is strong evidence that the intermediate, XII, does not contain a carbonyl or carboxyl group. That this highly strained bicyclic system would form at room temperature in water might at first appear unusual; however, a similar bicyclic system was isolated in the alternate synthesis of the N-substituted hydantoin (11).

### Conclusion

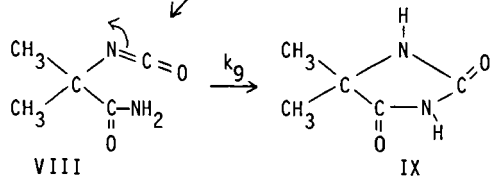
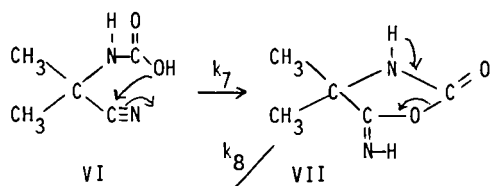
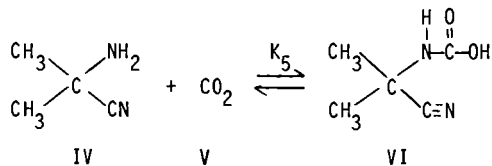
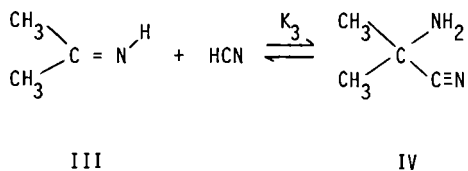
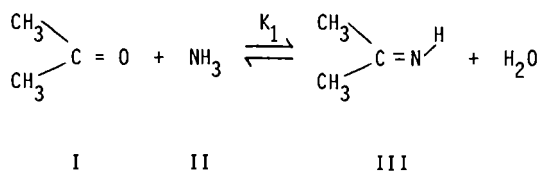
N-substituted hydantoin, specifically the N-(carbamyliisopropyl)-5,5-dimethylhydantoin, form in water at room temperature from the N- $\alpha$ -carbamyliisopropyl-N'- $\alpha$ -isobutyronitrile urea. Only a small amount of the 5,5-dimethylhydantoin, IX, is produced from the N-substituted urea, XI, or its carbamate salt, X. Thus, they are not likely intermediates in the formation of the DMH in water in the presence of acetone, hydrogen cyanide, carbon dioxide, and ammonia. Instead the hydantoin is believed to result from the hydrated conjugate base of the carbamic acid (VI) (Scheme 1).

### Acknowledgement

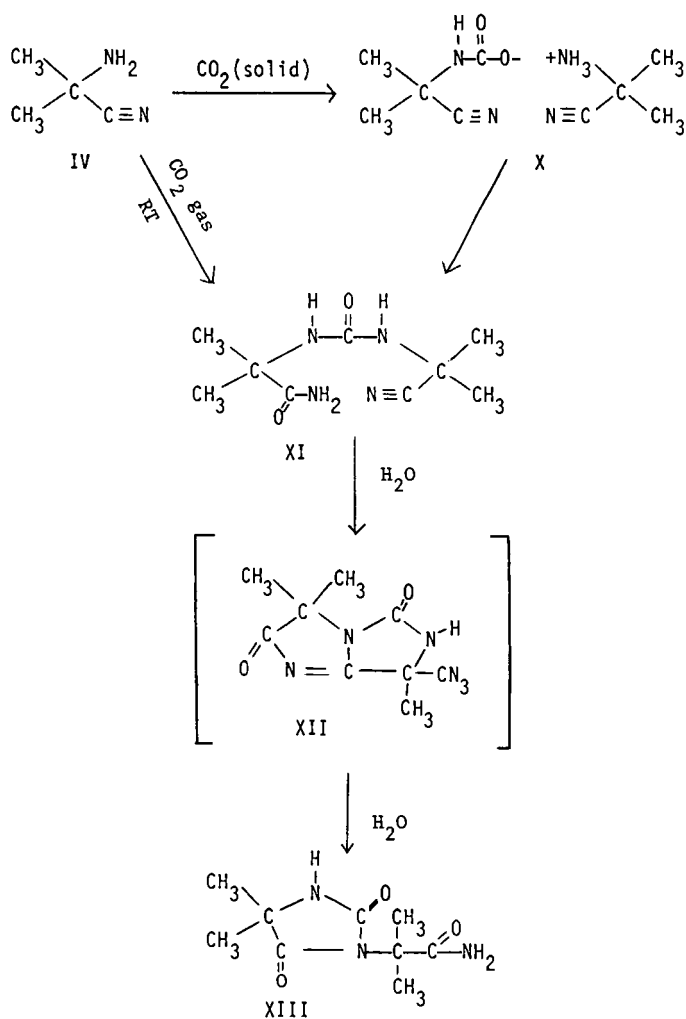
The advise of Dr. Warrack Willson, Manager of the Coal Conversion Research Division at the University of North Dakota Energy Research Center and the support from the U.S. DOE Grand Forks Project Office was appreciated.

### References

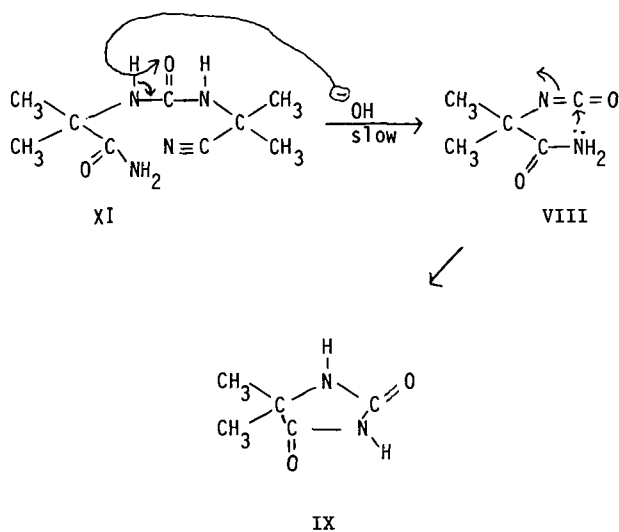
1. Ware, E. *Chem. Rev.*, 1950, **47**, 438.
2. Dorfman, R.I. "Encyclopedia of Chemical Technology", 3rd Ed., Vol. 12, John Wiley, NY, 1978, p. 692.
3. Olson, E.S., Diehl, J.W., and Miller, D.J. *Anal. Chem.*, 1983, **55**, 1111.
4. Mohr, D.H. and King, J.C., *Environ. Sci. Technol.*, 1985, **19**, 929.
5. Private Communication - Proprietary Information from Privately Owned International Gasification Corporations.
6. Olson, E.S., Worman, J.J., and Diehl, J.W. "The Formation of Hydantoin in Gasifier Condensate Water", *American Chemical Society Division of Fuel Chemistry Preprints*, 1985, **30** (2), 288.
7. Diehl, J., Olson, E., and Worman, J., *Fuel*, 1985, **64**, 1019.
8. Bucher, H.T. and Steiner, W.J., *J. Pract. Chem.*, 1934, **140**, 291.
9. Taillades, J. and Commeyras, A., *Tetrahedron*, 1974, **30**, 3407.
10. Rousset, A., Lasperas, M., Taillades, J., and Commeyras, A., *Tetrahedron*, 1980, **36**, 2649.
11. McKay, A.F., Paris, G.Y., and Garmaise, D.L., *J. Am. Chem. Soc.*, 1958, **80**, 6276.
12. Caplow N, *J. Am. Chem Soc.*, 1968, **90**, 6795 and references therein.
13. Nelson, D.A. and Worman, J.J., *Tetrahedron Letters*, 1966, 507.



Scheme 1. Mechanistic sequence for formation of DMH



Scheme 2. Mechanistic Pathway for the formation of the N-substituted hydantoin 3-( $\alpha$ -carbamyliisopropyl)-5,5-dimethylhydantoin (XIII)



Scheme 3. Possible mechanistic pathway for the formation of 5,5-Dimethylhydantoin from N- $\alpha$ -carbamylisopropyl-N'- $\alpha$ -isobutyronitrile urea (XI)

## LIQUID PHASE OXIDATION OF ALKYL SULFIDES AND THIOLS BY HYDROPEROXIDES

By

George W. Mushrush, Dennis R. Hardy, Harold G. Eaton  
and Robert N. Hazlett  
The Naval Research Laboratory  
Code 6180  
Washington, D. C. 20375

### INTRODUCTION

In general, jet fuels deteriorate in quality with time. One of the significant undesirable changes is the formation of insoluble material which can plug nozzles and filters and coat heat exchanger surfaces. Deposit formation in fuels is triggered by autoxidation reactions and is closely associated with hydroperoxide concentration (1-3). If the available oxygen is low and the temperature raised, the hydroperoxide concentration will be limited by free radical decomposition (2). This regimen (low oxygen and increasing temperature) is similar to the environment found in an aircraft fuel system.

The composition of deposits affords clues to the molecular species involved in deposit formation and the mechanism of formation. Hetero-atoms (oxygen, nitrogen and sulfur) and ash have been found to comprise up to 40% of such deposits (4-6). The sulfur content of these deposits has been found to vary from 1 to 9%. Sulfur (0.4% max. allowed) is the most abundant hetero-atom present in jet fuels.

This paper is concerned with the reaction between a primary autoxidation product, a hydroperoxide, and organo sulfides and thiols. Specifically, we examine the tert-butyl hydroperoxide oxidation of hexyl sulfide and dodecyl thiol in deaerated benzene at 120°C. The reactions were studied for time periods from 15 min to 180 min. Additionally, we have developed reaction conditions and an analytical method of high reproducibility which may be applicable to the study of other hydroperoxide oxidative processes.

### EXPERIMENTAL

Reagents tert-Butyl hydroperoxide, tBHP, (90%), hexyl sulfide and dodecyl thiol were obtained from Aldrich Chemical Co. They were distilled in vacuo to 99.9% purity. Benzene (Aldrich Gold Label) was refluxed and distilled from  $\text{CaH}_2$ .

**Method.** The reactions were carried out in sealed borosilicate glass tubes. The reagents (typically  $3\text{-}9 \times 10^{-4}$  mol of tBHP and  $6 \times 20^{-4}$  mole of hexyl sulfide or  $6 \times 10^{-4}$  mole of dodecyl thiol in 3.6 m mol of solvent) were weighed into 6 in. long, 1/4-in. o.d. Pyrex tubes closed at one end and fitted at the other with a stainless steel valve via a Swagelok (Teflon ferrules) fitting. The tube was attached to a vacuum system, cooled to 77K and subjected to several freeze-pump-thaw cycles. The tube was then subsequently flame-sealed below the valve. The ullage volume (0.30 ml) was kept constant for all runs. The deaerated samples were warmed to room temperature and immersed in a Cole-Parmer fluidized sand bath. The temperature (120°C) was controlled by a Leeds and Northrop Electromax III temperature controller. The total pressure during each run was estimated to be 5.1 atm for the runs in benzene. After the reaction period the sealed tube was quenched to 77K and opened. The tube was capped, warmed to room temperature and the internal standards added. The solution was transferred to a screw cap vial (Teflon cap-liner) and stored at 0°C until analysis. Since a typical chromatogram required 90 min, two internal standards were added. One, p-xylene, afforded quantitation for peaks with short retention times, and a second, 1-phenyltridecane, for the peaks with longer retention times.

Samples were heated for time periods of 15, 30, 60, 120 and 180 min except for those runs with the more reactive mercaptan (60 min max). All tubes were subjected to the same cleaning procedure. They were filled with toluene, cleaned with a nylon brush, rinsed with toluene twice, then with methylene chloride, and dried in air at 150°C for 8 h. A search of the literature gives a few examples of catalytic behavior with glass systems (7,8); however, when a glass tube was filled with crushed Pyrex, thus increasing the surface area, the results at 120°C for the above time periods were not substantially altered.

The samples were analyzed by two techniques, both based on gas chromatography. Peak identification for both techniques was based on retention time matching with standards and mass spectrometry. In the first, a Varian gas chromatograph Model 3700 with flame ionization detector (F.I.D.) and equipped with a 50-m 0.20-mm i.d. wall-coated open tubular (OV-101) fused silica capillary column gave the necessary resolution to distinctly separate the individual components. A carrier gas flow of 1 ml/min was combined with an inlet split ratio of 60:1, a temperature program with an initial hold at 50°C for 8 min and a ramp of 4°/min to a final temperature of 260°C.

In the second technique, gases formed during the reaction were analyzed using a Perkin-Elmer Model Sigma 2 gas chromatograph equipped with a 6-ft 5A Molecular Sieve column or a 4-ft Porapak/S column. For the gas analysis, the column was operated at 55°C. The chromatogram was recorded and integrated on a Hewlett-Packard Model 3390A reporting integrator. For this procedure, the valve was left on the reaction tube and after the appropriate reaction period, the tube valve was connected directly to a GC gas sampling valve via a Swagelok connection. An external standard was used for calibration. A pressure gauge measured the pressure in the sample loop at the time of analysis.

A material balance was assessed for each compound. The principal peaks of the chromatogram accounted for approximately 90% of the original compounds.

The very small peaks account for another 5-10%. The product distribution was repeatable to within 2-3% for each component.

## RESULTS AND DISCUSSION

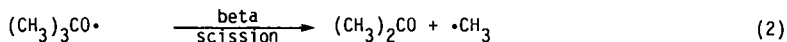
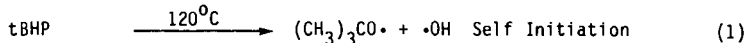
The thermal decomposition of an alkyl hydroperoxide is complex. At temperatures of 120°C or greater, tBHP decomposes by an autoinitiated pathway.<sup>9</sup> The major reaction pathway in the 120°C decomposition of tBHP, however, involves its attack by free radicals in the solution. The detailed mechanism of tBHP decomposition is highly dependent upon the specific reaction conditions employed since radical behavior is sensitive to structural, solvent and stereoelectronic effects.

The results in Table 1 illustrate that the product distribution from the reaction of tBHP with hexyl sulfide in deaerated benzene solvent can be conveniently divided into lower and higher molecular weight products. The quantities in Table 1 are based on per cent conversion from the moles of reactants originally present. Products derived solely from hexyl sulfide are calculated on the basis of the starting amount of hexyl sulfide. The tBHP derived products (for example, t-butanol) are similarly calculated based on the starting amount of tBHP. Mixed condensation products (i.e., tBHP + hexyl sulfide) are calculated on the basis of moles of hexyl sulfide. The values in Table 2 were likewise calculated using dodecyl thiol.

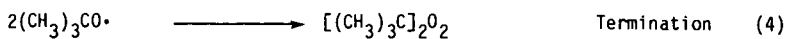
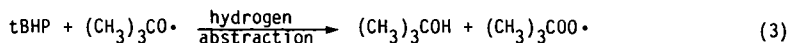
From tBHP, the major product was t-butanol. A small amount of acetone, methane, isobutylene and the tBHP radical termination product di-t-butylperoxide were also observed. From hexyl sulfide, lower molecular weight products included hexane, hexene and hexanal; higher molecular weight condensation products included the major product hexyl sulfoxide along with hexyl sulfone and hexyl disulfide. From dodecyl thiol, Table 2, lower molecular weight products included dodecane and dodecanol; higher molecular weight condensation products included the major product dodecyl disulfide along with dodecyl sulfoxide, dodecyl sulfide and dodecyl sulfone.

Solvent participation was noted by the formation of trace quantities of toluene and other substituted benzenes.

tBHP products The mechanism of autoinitiated tBHP decomposition can be depicted as follows:



Propagation



In aliphatic hydrocarbon solvent, it has been shown that beta-scission is favored over hydrogen abstraction at temperatures of 100°C or less. In the benzene solvent of this study, beta-scission was found to be less than competitive with hydrogen abstraction at 120°C. Small amounts of acetone were formed ranging from 1.5% for hexyl sulfide to 4.7% for dodecyl thiol at 60 min. By contrast, t-butanol was 75.4% for hexylsulfide and 76.7% for dodecyl thiol at 60 min. The greater yield of t-butanol compared to acetone definitively shows that hydrogen abstraction was favored over cleavage in benzene solvent under the conditions of this study. The increasing yield of acetone indicated, however, that at long reaction times beta-scission was a viable competing process.

Gaseous products The gaseous products formed included isobutylene, methane and a trace amount (0.1%) of ethane. No free oxygen was observed in any of the runs. As indicated in Table 1, isobutylene was 4.2% initially and decreased to 2.7% at 180 min. Methane increased from 0.8% at 15 min to 1.6% at 180 min. For dodecyl thiol, Table 2, isobutylene was 3.6% initially and decreased to 3.0% at 60 min. Methane increased from 0.9% at 15 min to 1.4% at 60 min.

Isobutylene probably resulted from the acid catalyzed dehydration of t-butanol. The decreasing yield was not surprising in light of the many pathways open to a reactive olefin in a radical environment.

The yield of methane was similar to that of acetone. This was an expected result since they both form via beta scission of the alkoxy radical (reaction 2). The reactive methyl radical easily abstracts hydrogen to yield methane rather than reacting with other radicals present in the system. This accounted for the low yield of methyl radical derived products.

The lack of measured oxygen does not mean that it was not formed. It could form from a non-terminating reaction of two t-butyl peroxy radicals and then be consumed immediately by any of several pathways.

Hexyl sulfide products The cleavage of a C-S bond in sulfides is known to occur in thermal and photochemical reactions.<sup>10</sup> The most direct means of generating a sulfur centered radical is the homolysis of a bond to sulfur. However, most simple alkyl sulfides are thermally quite stable (C-S bond dissociation energies are ca. 74 kcal/mol) and quite unreactive toward oxygen.<sup>11</sup> In the presence of t-butyl hydroperoxide, the t-butoxy radical generated was found to abstract the hydrogen alpha to the sulfur. Thus for hexyl sulfide, observed products were the thiyl radical and hexene. An alternate pathway would involve the attack of an alkoxy by a S<sub>H</sub>2 mechanism to yield both a thiyl radical and hexyl radical. That these processes were minor pathways can be seen from the results in Table 1. Hexane and hexene were present in low yields at all reaction times (hexane ca. 0.3% at 180 min and hexene 0.2%). Combination of thiyl radicals to form the disulfide was also a minor termination pathway (0.6% yield at 180 min).

Table 1

Mole % Conversion for the Reaction of Hexyl Sulfide with t-Butyl Hydroperoxide in Benzene Solvent at 120°C.

	Conversion (Mole %)				
	Reaction Time (min.)				
	15	30	60	120	180
<u>TBHP Products<sup>a</sup></u>					
Acetone	1.0	1.5	1.5	1.5	2.5
t-Butanol	55.5	59.5	65.9	69.8	75.4
di-t-butyl peroxide	0.5	0.7	0.7	0.7	1.0
<u>Hexyl sulfide Products<sup>b</sup></u>					
Hexene	0.1	0.1	0.1	0.3	0.2
Hexane	0.1	0.1	0.3	0.4	0.3
Hexanal	0.2	0.2	0.3	0.2	---
Hexyl disulfide	0.3	0.5	0.5	0.5	0.6
<u>Condensation Products<sup>b</sup></u>					
Hexyl sulfoxide	74.8	85.9	81.6	81.9	80.7
Hexyl sulfone	1.2	1.4	3.0	3.4	4.0
Hexyl thiosulfinate	0.1	0.1	0.1	0.1	---
<u>Gaseous Products</u>					
Methane	0.8	0.8	1.0	1.4	1.6
Isobutylene	4.2	3.9	3.6	3.1	2.7
<u>Unreacted</u>					
TBHP	28.9	23.9	8.7	3.9	1.8
Hexyl sulfide	22.5	13.9	8.2	3.9	2.9
<u>Trace Products<sup>c</sup></u>					
	6.7	7.8	9.7	10.1	8.1

a. based on the starting moles of TBHP

b. based on the starting moles of hexyl sulfide

c. summation of small peaks

The observed hexanal can be formed by several reaction pathways. Among these are the thermal rearrangement of the hexyl sulfoxide,<sup>12</sup> or more likely, the coupling of a t-butylperoxy radical with a thioacetal radical. Based on bond dissociation energy considerations alone, the t-butylperoxy radical was probably the least reactive and most plentiful radical present in the system.<sup>13</sup> This would favor a termination step involving this radical over a termination involving the very reactive alkoxy radical which would be expected to propagate the chain.

The major higher molecular weight product observed from the oxidation of hexyl sulfide by tBHP was hexyl sulfoxide. Its yield varied from 74.8% at 15 min. to 85.9% at 30 min., gradually decreasing to 80.7% at 180 min. of reaction. Other products included: hexyl sulfone (1.2% at 15 min. gradually increasing to 4.0% at 180 min.), hexyl disulfide (0.3 to 0.6%) and a trace amount of dihexyl thioisulfinate (0.1%).

Table 2

Mole % Conversion for the Reaction of Dodecyl Thiol with t-Butyl Hydroperoxide in Benzene Solvent at 120°C

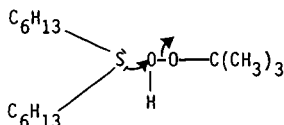
	Conversion (Mole %)		
	Reaction Time (min.)		
	15	30	60
<u>TBHP Products<sup>a</sup></u>			
Acetone	4.7	4.4	4.7
t-Butanol	59.2	65.4	76.7
di-t-butyl peroxid	1.6	1.6	1.9
<u>Dodecyl thiol Products<sup>b</sup></u>			
Dodecane	0.1	0.3	0.4
Dodecanal	0.6	0.7	1.1
Dodecyl sulfide	1.9	1.8	1.4
Dodecyl disulfide	74.4	78.8	74.1
<u>Condensation Products<sup>b</sup></u>			
Dodecyl sulfoxide	2.3	2.1	2.1
Dodecyl sulfone	0.9	1.5	1.7
<u>Gaseous Products</u>			
Methane	0.9	1.3	1.4
Isobutylene	3.6	3.3	3.0
<u>Unreacted</u>			
TBHP	19.7	12.6	1.3
Dodecylthiol	15.6	7.3	3.4
Trace Products <sup>c</sup>	4.6	6.7	9.4

a. based on the starting moles of TBHP

b. based on the starting moles of dodecyl thiol

c. summation of small peaks

The major product hexyl sulfoxide could result from at least two mechanisms: attack of oxygen-centered radicals (i.e., alkoxy) on sulfur followed by a beta scission;<sup>14</sup> or alternatively, the sulfoxide may arise from the reaction of t-butyl hydroperoxide with the hexyl sulfide.



The resulting sulfoxide once formed is quite stable, as can be seen from the slight lowering of the yield at extended reaction times.

The hexyl sulfone yield in the present work varied from an initial 1.2% at 15 min. to 4.0% at 180 min of reaction. This very slight increase compared to the yield of hexyl sulfoxide at 180 min. (80.7%) definitively illustrates the stability of the alkyl sulfoxide in the presence of tBHP.

The further oxidation of a sulfide or a sulfoxide to a sulfone is believed to proceed by a mechanism similar to that for sulfoxide formation from an alkyl sulfide.<sup>15</sup> The formation of an alkyl sulfone is a facile reaction only in the presence of a strong oxidant or when the reaction is catalyzed by transition metal ions.<sup>16</sup>

The hexyl disulfide product was a consequence of a self annihilation by dimerization of the thiyl radical. The thiyl radical was in low concentration at all reaction times (see hexyl termination products in the Table). As a result, the termination product hexyl disulfide was a minor product at all reaction times (1% at 180 min.). The other minor observed product forms as a direct result of the disulfide. The trace amounts of hexyl thiosulfinate observed (0.1% at all reaction times) resulted from the peroxidation of the disulfide.

**Dodecyl thiol products.** When thiols are oxidized by air or peroxides, disulfides are the major product regardless of the presence or absence of a catalyst.<sup>17</sup> The mechanism of thiol oxidation has been the subject of discussion for many years. Some reports support ionic mechanisms while others support radical processes.<sup>18</sup> The results in the present work, Table 2, support a radical mechanism. The t-butoxy radical generated from tBHP was found to abstract the thiol hydrogen. By contrast, hydrogen abstraction by the thiyl radical to yield a thiol is only observed in cases involving very stable thiyl radicals with active hydrogen donors.<sup>19</sup> Actually, the problem with this hydrogen abstraction is not that the process is slow, but that abstraction of a hydrogen from a thiol is thermodynamically favorable. Likewise, the thiyl radical has not been observed to undergo a beta scission to yield a thione and a methyl radical.<sup>20</sup> In the present work, thiones and thiols were not detected, even in trace amounts, in the product mix.

The observed secondary reaction products dodecane, dodecanal and dodecyl sulfide were present in low concentration for all reaction time periods. Dodecyl sulfide, 1.9% at 15 min decreasing to 1.4% to 60 min, was probably formed by the reaction of dodecyl thiol with the condensation product dodecyl sulfoxide. The products of such a reaction would be dodecyl disulfide and dodecyl sulfide. Dodecyl sulfide once formed could then undergo other side reactions. The observed dodecane was the result of such a reaction scheme: an  $S_H2$  reaction between the t-butoxy radical and dodecyl sulfide would result in both the dodecyl radical and a thiyl radical. The dodecanal product, 0.6% at 15 min increasing to 1.1% at 60 min, could result from several mechanisms. Among these are the thermal rearrangement of the sulfoxide or the coupling of the t-butyl peroxy radical with a thioacetal radical.

The major higher molecular weight product observed from the oxidation of dodecyl thiol by tBHP was dodecyl disulfide. Other products included dodecyl sulfoxide, dodecyl sulfone and trace but unreported amounts of dodecyl thiosulfinate.

Dodecyl disulfide, 74.4% at 15 min increasing to 78.8% at 30 min and then decreasing to 74.1% at 60 min, was formed by the direct oxidation of dodecyl thiol and subsequent dimerization of the thiyl radicals. An alternative side reaction for its formation would be the reaction of the

starting thiol with dodecyl sulfoxide to generate additional dodecyl disulfide.

The dodecyl sulfoxide, 2.3% at 15 min decreasing to 2.1% at 60 min, probably resulted from the same two pathways mentioned for hexyl sulfoxide.<sup>14</sup> The dodecyl sulfoxide yield was not observed to increase significantly due to further oxidation to dodecyl sulfone or for example its reaction with the starting thiol. The latter reaction would produce both dodecyl disulfide and dodecyl sulfide.

The low yield of dodecyl sulfone, 0.9% at 15 min increasing to 1.7% at 60 min, indicated the stability of alkyl sulfoxides toward further oxidation by tBHP in the liquid phase at 120°C.

#### LITERATURE CITED

1. Hazlett, R.N., Hall, J.M. and Matson, M., *Ind. & Eng. Chem. Prod. Res. Dev.*, **16**, 171 (1977).
2. Hazlett, R.N., "Frontiers of Free Radical Chemistry"; Academic Press: New York, (1980).
3. Taylor, W. and Wallace, T., *Ind. & Eng. Chem. Prod. Res. Dev.*, **6**, 258 (1967).
4. Cullis, C.F., Hirschler, M.M. and Rogers, R.L., *Proc. R. Soc. Lond, Ser. A* **375**, 543 (1981).
5. Rogers, J.D., SAE Meeting, Preprint 103T, Los Angeles, CA Oct. 5-9, (1959).
6. Nixon, A.C., "Autoxidation and Antioxidants"; Wiley: New York, Chap. 17 (1962).
7. Hiatt, R.R. and Irwin, K.C., *J. Org. Chem.*, **33**, 1436 (1968).
8. Mushrush, G.W. and Hazlett, R.N., *J. Org. Chem.*, **50**, 2387 (1985).
9. Howard, J.A., "The Chemistry of Functional Groups, Peroxides"; Wiley: New York, Chap. 8 (1983).
10. Calvert, J.G. and Pitts, J.N., "Photochemistry"; Wiley: New York, Chap. 5 (1966).
11. Correa, P.E. and Riley, O.P., *J. Org. Chem.*, **50**, 1787 (1985).
12. Barnard-Smith, D.G. and Ford, J.F., *Chem. Commun.*, **2**, 120 (1965).
13. Mushrush, G.W., Hazlett, R.N. and Eaton, H.G., *Ind. & Eng. Chem. Prod. Res. Dev.*, **24**, 290 (1985).
14. Rahman, A. and Williams, A., *J. Chem. Soc. (B)*, 1391 (1970).
15. Curci, R., Giovine, A. and Modena, G., *Tetrahedron*, **22**, 1235 (1966).
16. Henbest, H.B. and Khan, K.A., *Chem. Commun.*, **17**, 1036 (1968).
17. Wallace, T.J., *J. Org. Chem.*, **31**, 1217 (1966); cf. also Schrauzer, G.N. and Sibert, J.W., *J. Amer. Chem. Soc.*, **92**, 3509 (1970).
18. Cohen, S.G. and Aktipis, S., *J. Amer. Chem. Soc.*, **88**, 3587 (1966); cf. also Wagner, P.J. and Zepp, R.C., *ibid.*, **94**, 285 (1972).
19. Kice, J.L., "Free Radicals", Wiley: New York, Chap. 24 (1973).
20. VanSwet, H. and Kooyman, E.C., *Rec. Trav. Chim.* **87**, 45 (1968).

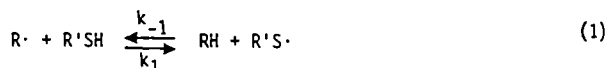
REACTIONS OF THE THIOPHENOXY RADICAL FROM THE  
THERMAL AND PHOTOLYTIC DECOMPOSITION OF PHENYLDISULFIDE

M. S. Alnajjar and J. A Franz

Pacific Northwest Laboratory  
P. O. Box 999  
Richland, WA 99352

INTRODUCTION

The importance of sulfur-containing constituents or additives on the thermal degradation of coal has been recognized by many investigators.<sup>1a-d</sup> Stock and co-workers<sup>1a,c</sup> in a study of the hydrogen atom transfer reactions of tetralin-d<sub>12</sub> with coal, diphenylmethane, and other coal model-compounds have shown that sources of thiol radicals such as benzylphenylsulfide significantly accelerate the rate of hydrogen shuttling between benzylic positions of model structures. Studies of deuterium exchange between deuterated donors and coals<sup>2a</sup> suggest that a higher sulfur content is correlated with a more rapid exchange of benzylic hydrogen with the deuterated donor. Activation barriers for abstraction of hydrogen atoms from thiols



( $k_1$ ) are less than a few kcal/mole, with the result that the reverse reaction, abstraction from hydrocarbons by thiol radical ( $k_{-1}$ ) is very rapid, being limited only by  $\Delta H^0$  of the reaction. For example, for R = benzyl and R' = phenyl in (eqn. 1)  $\log (k_1/M^{-1}s^{-1}) = (8.27 \pm 0.07) - (3.79 \pm 1.12)/\theta$ ,  $\theta = 2.3RT$  kcal/mole.<sup>2b</sup> For  $\Delta H^0 = -6.5$  kcal/mole,<sup>2c</sup>  $\log (k_{-1}/M^{-1}s^{-1}) = (8.5 \pm 0.5) - (10 \pm 2)/\theta$ . Thus, at coal liquefaction temperatures (450°C),  $k_1$  is about  $10^7 M^{-1}s^{-1}$  and  $k_{-1}$  is  $3 \times 10^5 M^{-1}s^{-1}$ , resulting in very rapid equilibration of hydrogen between benzylic sites. Rapid, reversible abstraction reactions of sulfur-centered radicals are well documented.<sup>3-8</sup> Hydrogen sulfide, pyrite, elemental sulfur, and organic disulfides have been suggested to play significant roles in promoting the liquefaction of various coals.<sup>1,9-12</sup> Displacement of aromatic substituents and dehydrogenation of hydroaromatic hydrocarbons facilitated by sulfur-centered radicals in reactions with sulfur and disulfides have been extensively studied.<sup>13-15</sup>

The rapid, reversible reactions of addition of sulfur-centered radicals to aromatic rings and readily reversible abstraction reactions (eqn.1) dominate mechanisms of structural evolution during liquefaction, by virtue of the weak S-S bond strengths of disulfides ( 54 kcal/mol for PhSSPh)<sup>16</sup> which assure that



the sulfur-centered radicals are present in significant concentrations throughout the coal liquefaction process for any sulfur-containing coal. Although it is well known that sulfur-sulfur bonds in alkyl and aryl disulfides and sulfides readily undergo photolytic or thermal homolysis, and many studies<sup>17-21</sup> have been devoted to the reactions of thiyl radicals with organic substrates, mechanistic aspects of the incorporation of sulfur into aromatic structure are perhaps less well developed, and detailed pathways of carbon-carbon and carbon-sulfur bond cleavage and formation reactions in the context of the thermal evolution of coal structure during liquefaction are lacking.

Thus, we present preliminary results of high-temperature reactions of phenyldisulfide and benzylphenyl sulfide with organic substrates (9,10-dihydroanthracene, diphenylmethane, bibenzyl, stilbene, and diphenylacetylene) which demonstrate mechanisms for the enhanced cleavage of  $\text{sp}^2\text{-sp}^2$ ,  $\text{sp}^2\text{-sp}^3$ , and  $\text{sp}^3\text{-sp}^3$  bonds mediated by thiophenoxy radical, and a series of addition-elimination, abstraction and rearrangement reactions leading to a series of thiophenes and related structures.

#### EXPERIMENTAL

General. NMR spectra were obtained with Varian FT-80 or Bruker AM-300 systems. Gas chromatography was performed with a Hewlett-Packard HP5890A instrument equipped with a 25-m, 0.32-mm i.d. J&W Scientific DB-5 capillary column. GC-mass spectrometry was performed with HP-5970 or HP-5992 systems. Products were identified by gc coinjection and comparison of mass spectra of authentic standards.

General Procedure for Thermolysis Reactions. In a typical reaction 0.05-0.10 mmole of phenyldisulfide or benzylphenylsulfide and an appropriate amount of

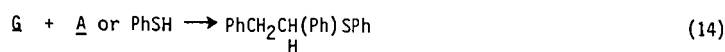
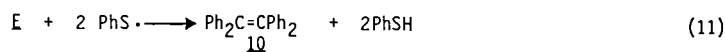
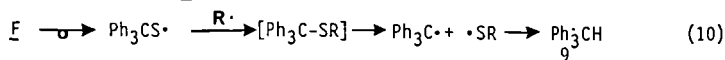
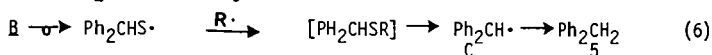
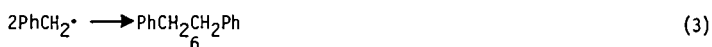
the desired additive were mixed in quartz tubes, freeze-thaw degassed, and sealed. The tubes were heated in a fluidized sand bath at  $400 \pm 5^\circ\text{C}$  for 30 min., cooled to room temp, opened under nitrogen, and transferred to a degassed methylene chloride solution containing naphthalene as an internal gc standard.

Thermolysis of Model Compounds in the Presence of Phenyldisulfide or Benzylphenylsulfide. Thermal decomposition of neat PhSSPh at  $400^\circ\text{C}$  produced the following products; thiophenol (1), diphenylsulfide (2), and thianthrene (3). Decomposition of neat benzylphenylsulfide produced the following products: toluene (4), 1, diphenylmethane (5), bibenzyl (6), 2, phenyldisulfide (7), 3, 2-phenylbenzothiophene (8), triphenylmethane (9) and tetraphenylethylene (10). The reactions of PhSSPh with additives are presented below, followed by major products in parentheses: PhSSPh + dihydroanthracene (1, 2, and anthracene); PhSSPh + diphenylmethane (1, 2, 4, 9 and 10); PhSSPh + bibenzyl (1, 2, 4, trans-stilbene (11), 8, 2,3-diphenylbenzothiophene (12), and 1,2,3,4-tetraphenylthiophene (13)); PhSSPh + trans-stilbene (1, 2, 4, 5, 8, 12, and 13); and PhSSPh + diphenylacetylene (1, 2, 4, 8, 12, and 13). The products listed accounted for typically 80% or more based on unrecovered starting material, with individual products varying from 5-10% to as high as 50%.

Preparation of 2,3-Diphenylbenzothiophene. Phenyldisulfide (0.50 mmol) and diphenylacetylene (0.50 mmol) were placed in a quartz tube, freeze-thaw degassed, and heated at  $400^\circ\text{C}$  for 30 min. The reaction mixture was transferred to hexane/ether solution (97/3 (v/v)) followed by flash liquid chromatography through a short silica column. Several fractions were taken for GC analysis. The fraction containing most of the product was concentrated. The residue was recrystallized from hexane to give 30% yield of 2,3-diphenylbenzothiophene:m.p.  $114-115^\circ\text{C}$  (lit.<sup>22</sup> 113-114). 300 MHz  $^1\text{H}$  NMR ( $\text{CDCl}_3$ ), 7.85 (m, 1H), 7.59 (m, 1H), 7.32 (m, 9H), 7.21 (m, 3H); 75 MHz  $^{13}\text{C}$  NMR ( $\text{CDCl}_3$ ), 140.87, 139.53, 138.84, 135.51, 134.22, 133.22, 130.42, 129.59, 128.62, 128.32, 127.67, 127.35, 124.50, 124.41, 123.33, 122.04; GC-MS, m/e (relative intensity) 287 (18,  $\text{M}^+ + 1$ ), 286 (100,  $\text{M}^+$ ), 285 (33), 284 (30), 282 (10), 271 (12), 252 (10), 44 (19).

## Results and Discussion

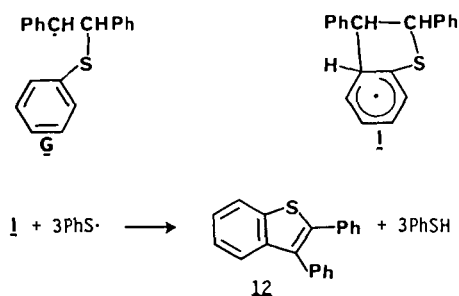
Pyrolysis of neat benzylphenylsulfide produced toluene, thiophenol,  $\text{Ph}_2\text{CH}_2$ ,  $\text{Ph}_2\text{S}_2$ ,  $\text{Ph}_3\text{CH}$ ,  $\text{Ph}_2\text{S}$ , 2-phenylbenzothiophene and 2,3-diphenylbenzothiophene. With a central bond strength of  $\approx 52 \pm 2$  kcal/mole,<sup>16</sup> benzylphenylsulfide will exhibit a unimolecular half-life of about 5 seconds at  $400^\circ\text{C}$ . The elementary free radical reactions in eqns. 2-14 show the origin of abstraction ( $\text{PhCH}_3$ ,  $\text{PhSH}$ ) rearrangement ( $\text{Ph}_3\text{CH}$ ,  $\text{Ph}_2\text{CH}_2$ ), and termination/oxidation ( $\text{Ph}_2\text{C}=\text{CPh}_2$ ,  $\text{PhCH}=\text{CHPh}$ ) products.



As noted, radical forming reactions for the weak C-S bonds (eqn. 2) are very rapid at 400°C resulting in the facile equilibria of eqns. 2 and 4.  $\text{Ph}_3\text{CH}$  and  $\text{Ph}_2\text{CH}_2$  both must occur via 1,2-aryl migration of phenyl from sulfur to carbon (equations 6,10), since an alternate mechanism of ipso displacement by benzyl radical on benzylphenylsulfide has been rendered unlikely based on other model studies.<sup>15,23</sup> Tetraphenylethylene (10) and stilbene (11) result from radical oxidation of the parent hydrocarbons  $\text{Ph}_2\text{CHCHPh}_2$  and  $\text{PhCH}_2\text{CH}_2\text{Ph}$ .

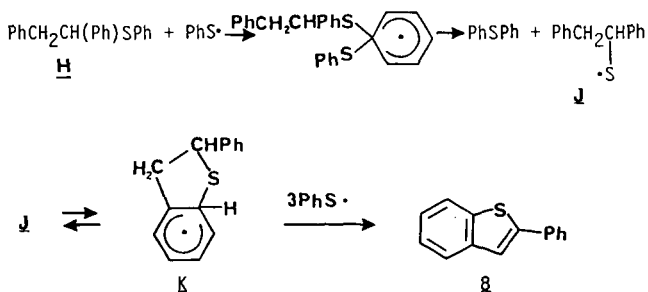
The formation of 2,3-diphenylbenzothiophene is a straightforward consequence of the formation of stilbene. Rapid, reversible addition of  $\text{PhS}\cdot$  to stilbene followed by cyclization and oxidation provides the observed product as shown in Scheme I.

Scheme I



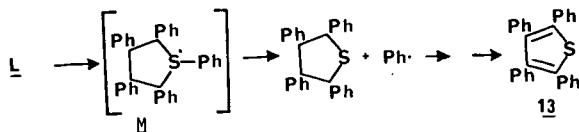
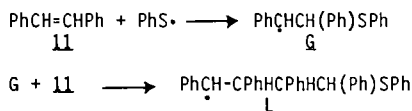
The formation of 2-phenylbenzothiophene must involve a displacement by the thiophenoxy radical on H as depicted in Scheme II.

Scheme II



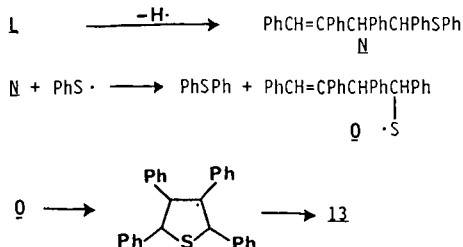
Oxidation of the intermediate hydrocarbons and radicals separating **K** and **G** will occur in straightforward fashion. The by-product  $\text{Ph}_2\text{S}$  was detected as a significant product accompanying the formation of **G**. The mechanisms of Schemes I and II were supported by products from reactions of stilbene and bibenzyl with  $\text{PhSSPh}$  at  $400^\circ\text{C}$ . Both reagents gave substantial yields of **12**. In addition, the reaction of stilbene and  $\text{PhSSPh}$  produced 1,2,3,4-tetraphenylthiophene (**13**). Scheme III depicts a plausible route for the formation of **13**. Displacement of a phenyl radical by the benzylic radical may proceed

Scheme III

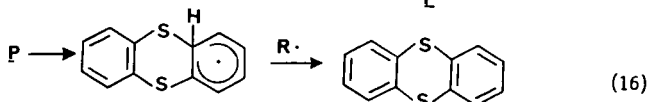
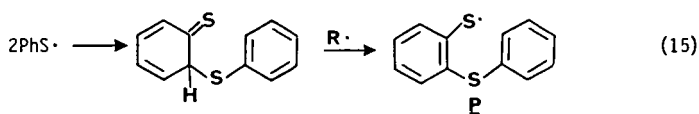


via the hypervalent 9-S-3 intermediate **M** lying in a shallow well of perhaps 3 kcal/mole,<sup>24</sup> or it may be merely a transition state. However, since displacement (although feasible at  $400^\circ\text{C}$ ) of the phenyl radical would be substantially endothermic, an alternate mechanism (Scheme IV) seems more likely.

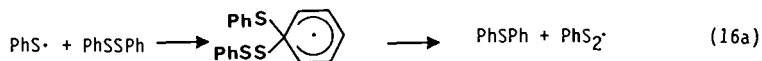
Scheme IV



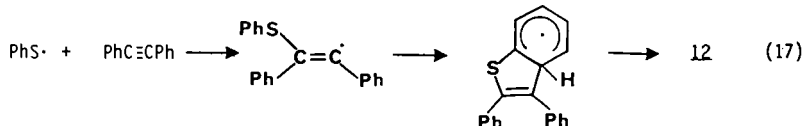
The displacement reaction of  $\text{PhS}\cdot$  with **11** will be rapid at these temperatures (cf. the photolysis of  $\text{Ph}_2\text{S}_2$  at  $25^\circ\text{C}$  efficiently produces  $\text{Ph}_2\text{S}$  as the major product), providing an unambiguous route to **13**. The thermolysis of neat phenyldisulfide provides thianthrene and phenylsulfide, the former product by a termination pathway (eqns. 15,16),



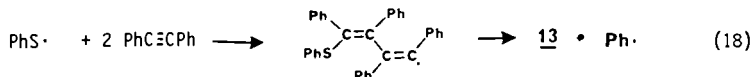
and the latter via direct displacement (eqn.16a).



The reaction of diphenylacetylene and  $\text{Ph}_2\text{S}_2$  produced 2,3-diphenylbenzothiophene in synthetically useful yields, along with **13**. Production of 2,3-diphenylbenzothiophene (**12**) occurs in straightforward fashion (eqn. 17).

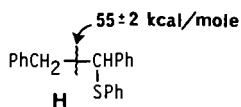


The formation of **13** is difficult to explain without proposing displacement by an intermediate vinylic radical at sulfur (eqn. 18). The displacement of



phenyl radical would be nearly thermoneutral in this case, and the 9-S-3 intermediate (or transition state) is quite plausible.

Finally, we note that significant yields of toluene were produced in reactions of stilbene and bibenzyl. The intermediacy of **H** is suggested.



The thermal C-C cleavage in H to produce  $\text{PhCH}_2\cdot$  and species B is expected to be rapid since the estimated bond dissociation energy is comparable to that of  $\text{PhSSPh}$  ( $55 \pm 2$  kcal/mol). The net effect of the thiophenoxy radical in these reactions will have been to substantially enhance the cleavage of  $\text{sp}^2\text{-sp}^2$  and  $\text{sp}^3\text{-sp}^3$  bonds in these otherwise refractory systems.

### Conclusions

The disulfide  $\rightleftharpoons$  thiophenoxy radical equilibrium, which models an important family of equilibrating sulfur-center radicals present during liquefaction of sulfur-containing coals, provides facile mechanisms for rapid hydrogen transfer, displacement and condensation reactions leading to enhanced cleavage of aralkyl structure on the one hand, and retrograde formation of nearly inert thiophene structures on the other hand. Further work is underway in this laboratory to determine the kinetics of 1,2-aryl migrations of phenyl from sulfur to carbon and to detect the intermediacy (if any), of 9-S-3 sulfur-centered radicals involved in radical displacement reactions at sulfur.

### Acknowledgment

This work was supported by the Office of Basic Energy Sciences, U.S. Department of Energy, under Contract De-AC06-76RLO 1830.

## References

- (a) Huang, C. B. and Stock, L. M., Prepr., Div. Fuel. Chem., Am. Chem. Soc. 1982, 27(3-4), 28.  
(b) Attar, A., Fuel 1978, 57, 201.  
(c) King, H.-H. and Stock, L. M., Fuel 1980, 59, 447.  
(d) Yarzab, R. F., Given, P. H., Spackman, W. and Davis, A., Fuel 1980, 59, 81.
- (a) Franz, J. A. and Camaioni, D. M. Fuel 1984, 63, 990.  
(b) Franz, J. A., Suleman, N. K. and Alnajjar, M. S., J. Org. Chem., in press.  
(c) Benson, S. W., "Thermochemical Kinetics, 2nd Ed.," Wiley-Interscience, New York, New York, 1976.
- Pryor, W. A., Gojon, G. and Stanley, J. P., J. Am. Chem. Soc. 1978, 43, 793.
- Walling, C. and Rabinowitz, R., J. Am. Chem. Soc. 1959, 81, 1137.
- Walling, C. "Free Radicals in Solution", Wiley-Interscience, New York, New York, 1957.
- Kellogg, R. M. "Methods in Free Radical Chemistry," E. S. Huysen, Ed., Marcel Dekker, New York, NY, Vol. II, 1969.
- Tanner, D. D., Wada, N. and Brownlee, B. G., Can. J. Chem. 1973, 51, 1870.
- Poutsma, M. L., "Free Radicals", (Ed. Kochi, J.), Wiley, New York, NY, Vol. II, 1973.
- Baldwin, R. M. and Vinciguerra, S., Fuel 1983, 62, 498.
- Abdel-Baset, M. and Ratcliffe, C. T. Prepr. Div. Fuel. Chem., Am. Chem. Soc. 1979, 25, 1.
- Sondreal, E. A., Wilson, W. G. and Stenberg, V. I., Fuel 1982, 61, 925.
- Takeya, G., Pure and Appl. Chem. 1978, 50, 1099.
- Glass, H. B. and Reid, E. E., J. Am. Chem. Soc. 1929, 51, 3428.
- Oae, S. and Kawamura, S., Bull. Chem. Soc. Jap. 1963, 36, 163.
- Ritter, J. J. and Sharpe, E. D., J. Am. Chem. Soc. 1937, 59, 2351.
- Benson, S. W., Chem. Rev. 1978, 78, 23.
- Sayamoi, K. and Knight, A. R., Can. J. Chem. 1968, 46, 999.
- Pryor, W. A. "Mechanisms of Sulfur Reactions." McGraw-Hill Book Co., New York, NY, 1962.
- Kice, J. L. "Free Radicals", (Ed. Kochi, J.), Wiley, New York, NY, 1973, Vol. II, Chap. 24.
- Smisman, E. E. and Sorenson, J. R. J., J. Org. Chem. 1965, 30, 4008.
- Walling, C. and Rabinowitz, R., J. Am. Chem. Soc. 1959, 81, 1137.
- Capozzi, G., Melloni, G. and Modena, G., J. Chem. Soc. (c), 1970, 2621.
- Poutsma, M. L., Fuel 1980, 59, 335.
- Beak, P. and Sullivan, T. A., J. Am. Chem. Soc. 1982, 104, 4450.

COAL LIQUEFACTION IN A FLUOROCARBON MEDIUM. II.  
KINETICS OF THE 1,2,3,4-TETRAHYDROQUINOLINE REACTION

Myron Kaufman, W. C. L. Jamison, S. Gandhi and Dennis Liotta

Department of Chemistry, Emory University, Atlanta, Georgia 30322

Introduction

Many coal liquefaction experiments involve heating coal in a medium which both reacts with the coal and simultaneously dissolves released coal fragments. One problem of this approach is that it is difficult to differentiate between physical interactions which result in solvent power and chemical reactions which disrupt the coal macromolecular network. A secondary problem of such experiments is that accurate measurements of coal conversion require considerable care in collecting all deposits adhering to the reactor walls.

We have reported that coal processed in a perfluorinated liquid medium with small amounts of additives does not dissolve, but in at least one case, that of 1,2,3,4-tetrahydroquinoline (THQ), the processed coal has considerably enhanced solubility. This increased solubility is attributed to a low temperature (200-250°C) reaction between THQ and coal. Since coal is recovered intact in these experiments, coal conversion can be measured by extraction of a fraction of the processed coal, without need for complete recovery of material from the reactor. In the present work, we present kinetic data in order to better understand the mechanism of this interesting coal transformation.

Experimental

These experiments were performed in FC-70 (3M Corp.), a mixture of perfluorinated tertiary aliphatic amines, with average molecular weight of 820 (primarily five-carbon chains), having a boiling point of 215°C. FC-70 has high solubility for gases such as H<sub>2</sub>, but very low room temperature solubility for both polar and nonpolar organic molecules. However, at temperatures greater than 200°C, the solubility of THQ in FC-70 exceeds the concentrations employed in the present studies. (FC-70 is not recommended for coal liquefaction experiments at T > 350°C, since at these temperatures the perfluorinated liquid decomposes and polymerizes.) Experiments were performed on three very different coals with carbon contents ranging from 74-84% (MAF). Properties of these coals, as suggested by the Pennsylvania State University Coal Bank, are given in Table 1. In the present work, representative samples of these coals, as obtained from the Coal Bank, are employed without preliminary grinding, washing or sieving. Reactions are carried out in stainless steel tubing bombs (15 cm x 1.3 cm o.d.). Typically the reactor contains 0.5 g of coal, 0.1 g of THQ and 12 g of FC-70. After sweeping out dissolved air, the reactor is pressurized with 8 MPa of H<sub>2</sub> and sealed with a high-pressure valve. The bombs are heated in a fluidized sand bath while being agitated at 300 cpm. Processed coals are compared on the basis of their pyridine solubility.

Table 1. Coal Properties

PSOC Designation	<u>1104</u>	<u>247</u>	<u>1098</u>
Moisture (%)	1.95	30.36	4.19
Ash (% on dry basis)	3.43	11.29	15.86
Volatile Matter (% MAF)	43.83	46.22	41.78
C (% MAF)	84.47	74.44	80.20
H (% MAF)	5.66	4.93	5.73
N (% MAF)	1.46	1.49	1.45
S (% MAF)	1.86	0.53	4.73
O (by difference)	6.48	18.61	7.89

1104 - HVA bituminous coal from Elkhorn #3 Seam

247 - North Dakota lignite A from Noonan Seam

1098 - Illinois #6 coal

After an 8-12 hour Soxhlet extraction with acetone, the processed coals contain only 3-4% retained THQ (from nitrogen analysis). The light color of the acetone extract indicates that very little of the coal is removed in this step. Pyridine extraction was for a minimum of 8 hours in a micro-Soxhlet apparatus, followed by two-hour extractions with benzene and acetone, a procedure found necessary to remove adhered pyridine from the coal.<sup>1-3</sup> All weighings were done after an 8-hour vacuum drying at 110°C followed by equilibration with CaSO<sub>4</sub> in a desiccator.

### Results

Coal heated at 250°C in FC-70 with low concentrations of THQ visually appears the same as untreated coal. After the coal particles settle, the FC-70 is transparent and uncolored. It is found, however, that the pyridine solubility of treated coal is increased substantially over its original value. As shown in Figure 1, the conversions of the three very different coals all asymptotically approach 33-35% in long (18 hour) runs, with no evidence of char formation, as indicated by decreased conversion at long time. The pyridine solubilities of the unprocessed coals are included as the t=0 points on these curves. To within the scatter of the data, the plots of  $\log(C(\infty) - C(t))$  vs time, shown in Figure 2, are straight lines, in agreement with first-order approach to the ultimate conversions obtainable in these experiments. The least-squares slopes and correlation coefficients of these lines are:  $-.62\text{hr}^{-1}$ ,  $-.98$  (1104),  $-.77\text{hr}^{-1}$ ,  $-.99$  (247), and  $-.57\text{hr}^{-1}$ ,  $-.95$  (1098). These slopes are reasonably close. However, the lignitic coal (247) has very low unprocessed solubility, and undergoes a rapid initial increase in conversion to a value similar to those of the other two coals. If the unprocessed conversion of PSOC 247 coal is not included in the least-squares analysis,<sup>1</sup> the slope of its approach to ultimate solubility is even closer ( $-.70\text{hr}^{-1}$ ,  $-.999$ ) to the slopes for the other two coals.

### Discussion

Most coal liquefaction studies emphasize variations in behavior between different coals. In this work we have demonstrated a mode of processing in which three very different coals approach almost identical ultimate conversions

at similar rates. The range of first-order rate constants for the three coals is 30% of their mean value. However, if the unprocessed value ( $t = 0$ ) is not included in calculating the rate for the lignitic coal (PSOC-247), the range is only 20%. We have previously noted,<sup>1</sup> that it is relatively easy to induce small increases in the conversion of PSOC-247, perhaps because it is initially only 4% soluble in pyridine. For example, unlike a bituminous coal, the conversion of PSOC-247 increased 8% when quinoline rather than THQ is used in our experiment. Thus, it is likely that after an initial very rapid increase in conversion of PSOC-247, its approach to ultimate solubility is at a rate very close to that of the higher rank coals. These kinetics appear to be representative of a chemical reaction rather than of mass transport, since there is very little change in the rate of coal conversion when a fine sieved fraction of the coals is processed. (PSOC-1104, 100-200  $\mu$  particles, compared to the as-received coal, which has > 50% of its mass in particles larger than 400  $\mu$ .)

There are a number of reasons for preferring a mechanism for these observations that is based on breaking chemical bonds in the coal macromolecular network, rather than one based on physical effects, such as swelling due to relaxation of hydrogen bonds. First, physical effects are generally reversible,<sup>4</sup> and we measure coal conversion after almost all the THQ is removed by 12-hour acetone extraction and the acetone is removed by drying at 110°C, a procedure which should allow reformation of hydrogen bonds. Second, when shorter acetone washes are employed, leaving ca. twice as much THQ on the coal, very similar results are obtained,<sup>5</sup> whereas additional hydrogen-bond rupture would be anticipated with more adsorbed THQ. Third, using the strong bases triethylamine and ethylenediamine in place of THQ produces less than 5% increase in conversion (bituminous coals for 4½ hours). Ethylenediamine is a particularly good low-temperature solvent for coal,<sup>3,6</sup> and would be expected to be effective in a purely physical mechanism. Last, NMR spectra of the evaporated acetone wash show considerable conversion of THQ to quinoline in these experiments. Without H<sub>2</sub> for reformation of THQ, conversions are somewhat reduced.<sup>1</sup> Although probably only a small fraction of the hydrogen transferred from THQ breaks bonds in the coal macromolecule, observation of THQ conversion is consistent with the chemical reaction mechanism. These four points provide a strong argument for a low temperature reaction between THQ and the macromolecular network of a variety of coals and offer an explanation for the unique efficacy of THQ as a coal liquefaction medium.

Although dehydrogenation of THQ is observed in this work, tetralin, another potent hydrogen donor, does not increase coal solubility in similar experiments. Thus, neither basicity nor hydrogen donor ability alone is sufficient for the liquefaction reaction, and it appears that the proximity of a lone pair of electrons to a labile hydrogen is necessary. There are model compounds, such as diphenyl disulfide, which are related to weak bonds in proposed coal structures,<sup>7</sup> and react with THQ at 250°C. It is not yet known, however, which of these reactions satisfy the other criteria (kinetics, selectivity against tetralin, etc.) necessary to explain the results of our experiments. Experiments are continuing to further explore the parameters of this process and to find a mechanism to describe it.

#### Acknowledgment

This work has been supported by the U. S. Department of Energy under contract DE-FG22-82PC50785. A grant from the Emory University Research Committee is also acknowledged. Provision of perfluorocarbon materials by 3M Corporation is greatly appreciated.

#### References

1. Kaufman, M., Jamison, W. C. L. and Liotta, D., Fuel 65, 148 (1986).
2. Derbyshire, F. J., Odoerfer, G. A. and Whitehurst, D. D., Fuel 63, 56 (1984).
3. Collins, C. J., Hagaman, E. W., Jones, R. M. and Vernon, F. R., Fuel 60, 359 (1981).
4. Brenner, D., Nature 306, 772 (1983).
5. Dryden, I. G. C., Fuel 30, 39 (1951).
6. VanBodegom, B., vanVeen, J. A. R., vanKessel, G. M. M., Sinnige-Nijssen, M. W. A. and Stuiiver, H. C. M., Fuel 64, 59 (1985).
7. Whitehurst, D. D., Mitchel, T. O. and Farcașiu, M., Coal Liquefaction, Academic Press (1980) p. 22.

Figure 1. Coal Conversion with THQ in FC-70

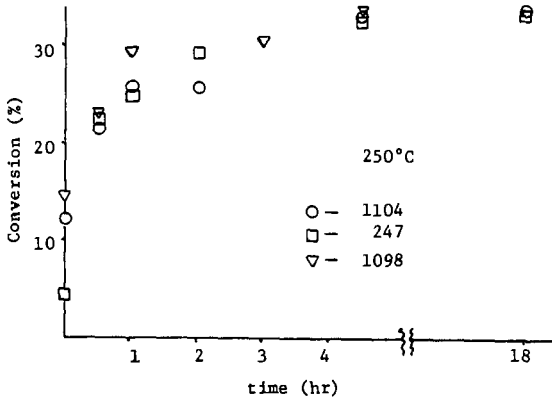
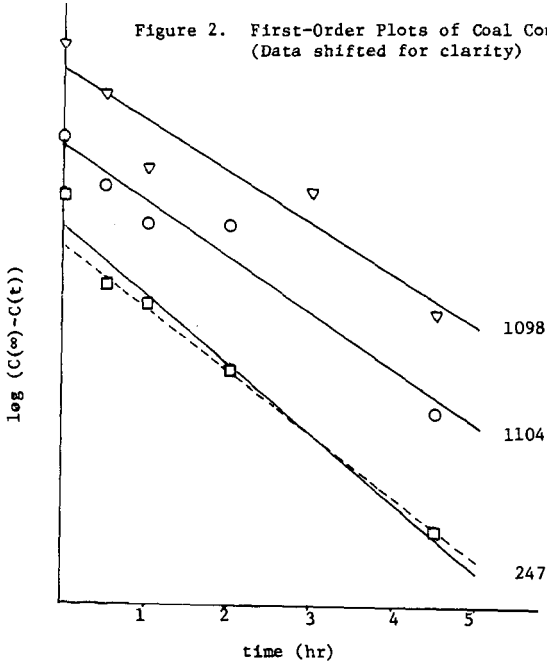


Figure 2. First-Order Plots of Coal Conversion (Data shifted for clarity)



## LIQUEFACTION CO-PROCESSING OF COAL AND SHALE OIL

R. L. Miller

Chemical Engineering Department  
University of Wyoming  
Laramie, Wyoming 82071

### ABSTRACT

Results are reported for a series of experiments in which Wyodak subbituminous coal and shale oil derived from medium grade Colorado shale were co-processed at typical coal liquefaction reaction conditions. Distillate yields in excess of 60 wt% MAF coal with corresponding hydrogen consumption values of less than 2.8 wt% MAF coal were obtained in a once-through process configuration. Encouraging results were also obtained from low severity experiments using CO/H<sub>2</sub>O rather than H<sub>2</sub> as reducing agent. Prehydrotreatment of the shale oil, feed coal reactivity, and use of a disposable catalyst were shown to affect process performance.

### INTRODUCTION

A number of studies have been reported in which coal and non-coal-derived heavy solvents were simultaneously converted to more valuable distillable liquid products (1 - 6). This type of once-through process, known as co-processing or liquefaction co-processing, has several potential advantages over conventional direct liquefaction:

- Two low grade feeds are converted to higher quality liquid products.
- Recycle solvent requirements are reduced or eliminated resulting in lower capital investment and operating costs.
- Existing petroleum refinery capacity can be utilized with minimal process modification.

However, liquefaction co-processing does suffer from a number of technical problems which must be solved before commercial development can proceed. Most non-coal-derived heavy oils derived from petroleum, oil shale, or tar sands are less aromatic than coal-derived liquids, and, not surprisingly, have been shown to be rather poor coal dissolution solvents. Typically, very severe thermal reaction conditions and/or use of expensive heterogeneous catalysts are utilized during co-processing to obtain sufficiently high levels of coal conversion. This generally results in excessive hydrogen consumption and cracking of distillable liquids to gases.

An alternate approach to the problem of increasing coal dissolution has been employed in the present study. Results of exploratory liquefaction co-processing experiments demonstrated that selected non-coal-derived heavy oils, each with a nitrogen content in excess of about 1.2 wt%, could be used to dissolve Wyodak subbituminous coal at typical coal liquefaction reaction conditions (7). This effect was not surprising, since quinoline-type nitrogen compounds such as tetrahydroquinoline (THQ) have been shown to greatly enhance coal dissolution in model compound studies (8 - 10). Based on encouraging results from the exploratory screening runs, additional co-processing studies using promising coal/heavy oil combinations were undertaken.

The objective of this paper is to report yield and conversion results from liquefaction co-processing experiments using Wyodak subbituminous coal and shale oil

derived from medium grade Colorado shale. Runs designed to demonstrate the effects of feed coal reactivity, mild hydrotreatment of feed shale oil prior to co-processing, and use of hydrogen or carbon monoxide/water as feed gas were included in this study.

#### EXPERIMENTAL PROCEDURE

Wyodak subbituminous coal samples Wyo-1 and Wyo-3 were used as feed coals in the liquefaction co-processing experiments. Ultimate analyses for these samples are presented in Table I. Sampling and preparation details of the coals have been reported elsewhere (11, 12). Previous reactivity studies performed on four Wyodak subbituminous coals including Wyo-1 and Wyo-3 indicated that Wyo-3 coal was an extremely reactive coal at representative direct liquefaction reaction conditions (11, 13). The high degree of reactivity was primarily attributed to the high organic sulfur and reactive maceral (vitrinite and exinite) contents of Wyo-3 coal. Wyo-1 coal was found to be much less reactive at liquefaction reaction conditions. Coal samples were dried to less than 1.0 wt% moisture content before use in the liquefaction co-processing experiments.

Two shale oil samples were used in the liquefaction co-processing runs. Solvent A-5 was a full boiling range sample of shale oil obtained from the Western Research Institute (formerly the Laramie Energy Technology Center of the Department of Energy). This sample was produced from thermal retorting of medium grade (29 gal/ton) Colorado oil shale. Solvent A-6 was prepared by mildly hydrotreating a portion of sample A-5 in a two liter batch Autoclave Magnedrive II reactor at 650°F for one hour with an initial cold hydrogen pressure of 2000 psig. Nalco 477 cobalt molybdate catalyst was used to hydrotreat the shale oil. Catalyst samples were thermactivated at 1000°F for two hours in a muffle furnace prior to use. Approximately 0.6 wt% hydrogen was consumed by the shale oil during hydrotreating. Properties of shale oil samples A-5 and A-6 are presented in Table II. Approximately 50 wt% of the nitrogen in these samples existed in quinoline-type or hydroquinoline-type molecular structures.

Iron oxide provided by the Kerr-McGee Corporation and carbon disulfide were used as disposable catalysts in some co-processing runs using hydrogen as feed gas. Each of these materials was added to the reaction mixture in an amount equal to 5 wt% of the dry feed coal. Iron sulfate (5 wt% MF feed coal) was used as catalyst in selected CO/H<sub>2</sub>O experiments.

The liquefaction co-processing experiments were carried out in a 60 cm<sup>3</sup> stirred microautoclave reactor system designed and constructed at the University of Wyoming. The reactor was similar to larger Autoclave batch reactors except that heating was accomplished with an external high temperature furnace. At the end of each run, the reactor and its contents were quenched with an icewater batch. This reactor system provided the benefits of small tubing bomb reactors [quick heatup (~2 min. from room temperature to 850°F) and cooldown (~30 sec. back to room temperature)], while at the same time insuring sufficient mechanical agitation of the reactants with an Autoclave Magnedrive II stirring assembly to minimize hydrogen mass transfer effects. The system was also designed so that the reactor pressure was very nearly constant throughout an experiment. Two iron-constantan thermocouples attached to a Fluke 2175A digital thermometer were used for temperature measurements. One thermocouple measured the temperature of the reactor contents, while the other measured the temperature of the reactor wall. Reactor pressure was monitored using a 0 - 5000 psi Marsh pressure gauge.

A majority of the liquefaction co-processing runs were completed at representative coal liquefaction reaction conditions: 825°F reaction temperature, 2000 psig initial cold hydrogen pressure, and 30 or 60 minutes reaction time. Some preliminary experiments were also completed at more mild reaction conditions using carbon

monoxide and water rather than hydrogen as the reducing agent. In these runs, hydrogen was produced from CO and H<sub>2</sub>O via the water gas shift reaction. The CO/H<sub>2</sub>O runs were completed at 600°F reaction temperature, 1500 psig initial cold carbon monoxide pressure, and 30 minutes reaction time. Distilled water in an amount equal to 50 wt% of the dry feed coal was added to runs using a carbon monoxide atmosphere.

Gaseous products were analyzed using gas chromatography. Water and distillate yields were measured by distilling portions of the combined liquid-solid product mixture to an 850°F endpoint in a microdistillation apparatus. Additional portions of the liquid-solid product mixture were extracted in a Soxhlet extraction apparatus using cyclohexane, toluene, and pyridine. Details of the experimental procedures used in this work have been reported (7).

## RESULTS AND DISCUSSION

Using data collected with the analytical procedures described, detailed yield and conversion results were computed for each liquefaction co-processing run. Details of the computational methods used in this study have been described previously (7). For purposes of the present discussion, process performance will be monitored using the following three parameters: C<sub>4</sub>-850°F distillate yield (wt% MAF coal basis), hydrogen utilization efficiency, and pyridine conversion (wt% MAF basis). Hydrogen utilization efficiency is defined as the mass of C<sub>4</sub>-850°F distillate produced per unit mass of hydrogen consumed. The value of this parameter provides a good indication of the overall efficiency of hydrogen consumed in the co-processing experiments. Pyridine conversion is defined as a measure of the extent of conversion of all feeds (coal and non-coal-derived heavy oil) to pyridine soluble products. However, since both A-5 and A-6 shale oil samples were completely soluble in pyridine, the pyridine conversion values reported in this paper are direct measures of the extent of coal conversion in the co-processing runs.

### Effect of Shale Oil Prehydrotreatment

The results from liquefaction co-processing experiments using Wyo-3 coal and A-5 or A-6 shale oil at 825°F and 2000 psig initial cold hydrogen pressure are shown in Figures 1 - 3. It is apparent from this data that mild prehydrotreatment of the shale oil prior to co-processing greatly enhances process performance. Distillate yields of 55 - 60 wt%, hydrogen utilization efficiencies of about 20, and pyridine coal conversion values of 68 - 85 wt% were obtained using Wyo-3 coal and A-6 shale oil. Similar enhancement effects were seen using Wyo-1 feed coal. Previous co-processing studies by Kerr-McGee using Ohio No. 5 bituminous coal and Canadian Cold Lake bitumen also demonstrated the beneficial effect of heavy oil hydrotreatment prior to co-processing (14).

At least two possible reasons exist for the effects shown in Figures 1 - 3. First, mildly hydrotreated A-6 shale oil acted as a more powerful hydrogen donor solvent than A-5 in promoting coal conversion and distillate production. Secondly, the quinoline-type nitrogen content of A-5 was approximately 0.7 wt%. Mild hydrotreatment of A-5 presumably converted a number of the quinoline structures to hydroquinoline structures. As mentioned earlier in this paper, hydroquinolines such as tetrahydroquinoline (THQ) have been shown to actively promote coal solvation in direct liquefaction. The data shown in Figures 1 - 3 suggest that a similar effect occurred during liquefaction co-processing with A-6 shale oil.

### Effect of Feed Coal Reactivity

Figure 4 presents a comparison of yield results for co-processing runs using Wyo-1 and Wyo-3 coal. These data show that liquefaction co-processing performance is a strong function of feed coal reactivity as measured by the extent of dissolution to

pyridine solubles and distillate production. As shown in Figure 5, the detrimental effects of low feed coal reactivity can be partially offset by use of a disposable catalyst such as iron oxide/carbon disulfide.

#### Liquefaction Co-Processing Using Carbon Monoxide and Water

Several previous studies have reported the successful liquefaction of low rank coal at mild reaction conditions using carbon monoxide and water in place of hydrogen gas (5, 15, 16). In these runs, hydrogen was provided by the water gas shift (WGS) reaction involving carbon monoxide and water. In the aqueous phase, a number of catalysts such as alkali metal salts, alkaline earth salts, and organic nitrogen bases have been shown to catalyze the WGS reaction (17).

Hypothesizing that the high basic nitrogen content of A-6 shale oil would also catalyze the WGS reaction, several preliminary liquefaction co-processing experiments using Wyo-3 coal, A-6 shale oil, and CO/H<sub>2</sub>O were completed. As shown in Figure 6, significant conversion of coal and 850°F<sup>+</sup> shale oil to distillate liquids was obtained, even though the reaction conditions were very mild. Use of iron sulfate as a disposable catalyst provided some improvement in yield structure and coal conversion. Based on these encouraging results, a more extensive study of liquefaction co-processing using carbon monoxide and water is underway.

#### CONCLUSIONS

A series of liquefaction co-processing experiments has been completed using two Wyodak subbituminous coals and two shale oil feeds. Both hydrogen and carbon monoxide/water were evaluated as reducing agents. Results indicated that prehydro-treatment of the shale oil, feed coal reactivity, and to some extent, use of a disposable catalyst all affect process performance. Sample A-6 was found to be an attractive feedstock for liquefaction co-processing. Distillate yields in excess of 60 wt% MAF coal were obtained using Wyo-3 coal and A-6 shale oil at typical coal liquefaction conditions. Encouraging results were also obtained using CO/H<sub>2</sub>O at much more mild reaction conditions.

#### ACKNOWLEDGEMENTS

Financial support for this research was provided by the Electric Power Research Institute under Contract Number RP 2383-01. Mr. Conrad Kulik of EPRI provided helpful comments.

#### REFERENCES

1. Yan, T.Y., and Espenscheid, W.F., *Fuel Proc. Tech.*, 7, 121, (1983).
2. Shinn, J.H., Dahlberg, A.J., Kuehler, C.W., and Rosenthal, J.W., "The Chevron Co-Refining Process," *Proceedings of the Ninth Annual EPRI Contractors' Conference on Coal Liquefaction*, Palo Alto, California, (May 1984).
3. Kelly, J.F., Fouda, S.A., Rahimi, P., and Ikura, M., "CANMET Coprocessing: A Status Report," *CANMET Coal Conversion Contractors' Review Meeting*, Calgary, Alberta, Canada, (November 1984).
4. Curtis, C.W., Guin, J.A., Pass, M., and Tsai, K.J., *ACS Fuel Chem. Preprints*, 29, 5, 155, (1984).
5. Ignasiak, B., Kovacik, G., Ohuchi, T., Lewkowicz, L., and duPlessis, M.P., "Two-Stage Liquefaction of Subbituminous Alberta Coals in Non-Donor Solvents," *CANMET Coal Conversion Contractors' Review Meeting*, Calgary, Alberta, Canada, (November 1984).

6. Miller, R.L., "Use of Non-Coal-Derived Heavy Solvents in Direct Coal Liquefaction," Proceedings of the Tenth Annual EPRI Contractors' Conference on Coal Liquefaction, Palo Alto, California, (April 1985).
7. Miller, R.L., "Use of Non-Coal-Derived Heavy Solvents in Direct Coal Liquefaction," Interim Report for EPRI Project RP 2383-01, (November 1985).
8. Atherton, L.F., and Kulik, C.J., "Advanced Coal Liquefaction," presented at the 1982 AIChE Annual Meeting, Los Angeles, California, (November 1982).
9. McNeil, R.I., Young, D.C., and Cronauer, D.C., Fuel, 62, 806, 1983.
10. Broderick, T.E., "Liquefaction of Wyodak Coal in Tetrahydroquinoline," M.S. Thesis, University of Wyoming, Laramie, Wyoming, (1984).
11. Miller, R.L., "Effect of Wyodak (Wyoming) Coal Properties on Direct Liquefaction Reactivity," Ph.D. Dissertation, Colorado School of Mines, Golden, Colorado, (1982).
12. Silver, H.F., Corry, R.G., and Miller, R.L., "Coal Liquefaction Studies," Final Report for EPRI Projects RP 779-23 and RP 2210-1, (December 1982).
13. Miller, R.L., and Baldwin, R.M., Fuel, 64, 1235, (1985).
14. Rhodes, D.E., "Comparison of Coal and Bitumen-Coal Process Configurations," Proceedings of the Tenth Annual EPRI Contractors' Conference on Coal Liquefaction, Palo Alto, California, (April 1985).
15. Ross, D.S., Blessing, J.E., Nguyen, Q.C., and Hum, G.P., Fuel, 63, 1206, (1984).
16. Hodges, S., and Creasy, D.E., Fuel, 64, 1229, (1985).
17. Elliott, D.C., and Sealock, L.J., I & EC Proc. Des. Dev., 22, 426, (1983).

Table I  
Ultimate Analysis of Wyodak Subbituminous Coal Samples

Sample	<u>Wyo-1</u>	<u>Wyo-3</u>
Ultimate Analysis, wt% dry basis		
Carbon	69.8	58.2
Hydrogen	4.7	4.3
Nitrogen	0.8	0.8
Sulfur	0.3	2.9
Sulfate	0.0	0.8
Pyrite	0.0	0.9
Organic	0.3	1.2
Oxygen (difference)	18.3	13.9
Ash	6.1	19.9

Table II  
Properties of Shale Oil Samples

Sample	<u>A-5</u>	<u>A-6</u>
Wt% Distilled		
Water	0.7	0.1
350°F	4.2	10.3
350°-500°F	9.6	18.3
500°-650°F	18.8	22.5
650°-850°F	39.0	29.8
850°F+	27.7	19.0
Ultimate Analysis, wt% dry basis		
Carbon	83.3	84.7
Hydrogen	12.1	12.9
Nitrogen	1.4	1.2
Sulfur	0.5	0.4
Oxygen (difference)	2.7	0.8
Ash	0.0	0.0

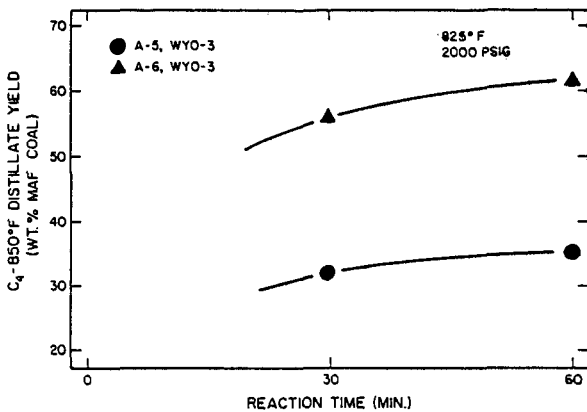


Figure 1. Distillate Yield as a Function of Reaction Time and Shale Oil Feed

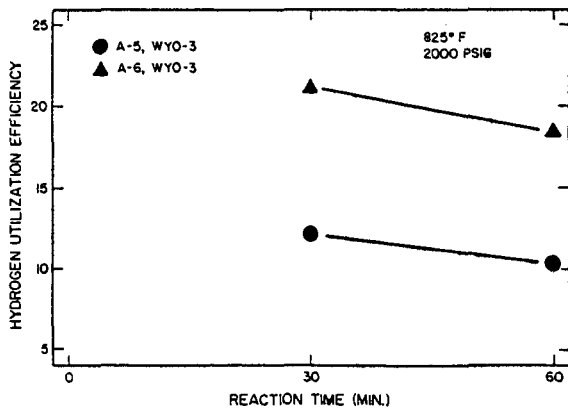


Figure 2. Hydrogen Utilization Efficiency as a Function of Reaction Time and Shale Oil Feed

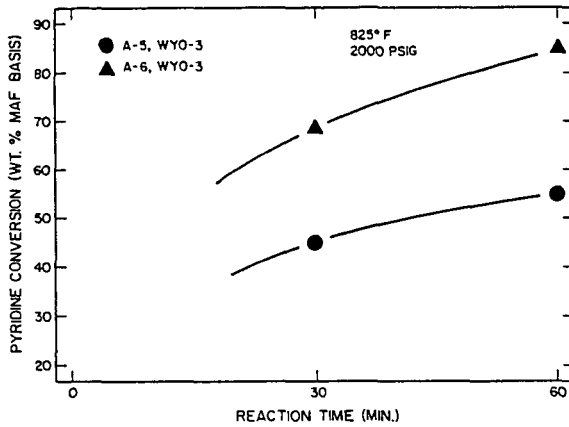


Figure 3. Pyridine Conversion as a Function of Reaction Time and Shale Oil Feed

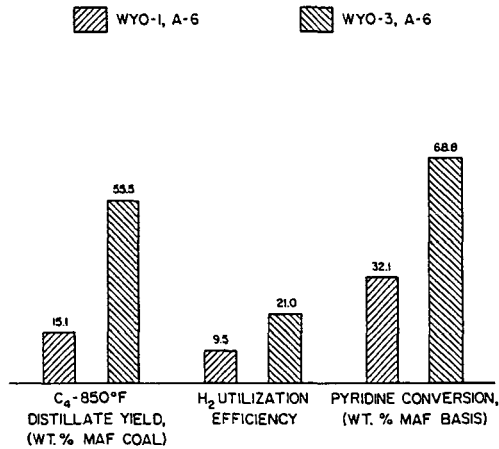


Figure 4. Effect of Feed Coal Reactivity on Process Performance (Reaction Conditions: 825°F, 2000 psig H<sub>2</sub>, 30 min.)

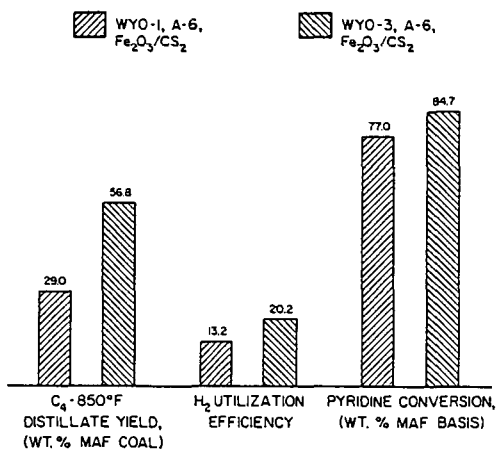


Figure 5. Effect of Feed Coal Reactivity on Process Performance (Reaction Conditions: 825°F, 2000 psig H<sub>2</sub>, 30 min., Fe<sub>2</sub>O<sub>3</sub>/CS<sub>2</sub> Catalyst)

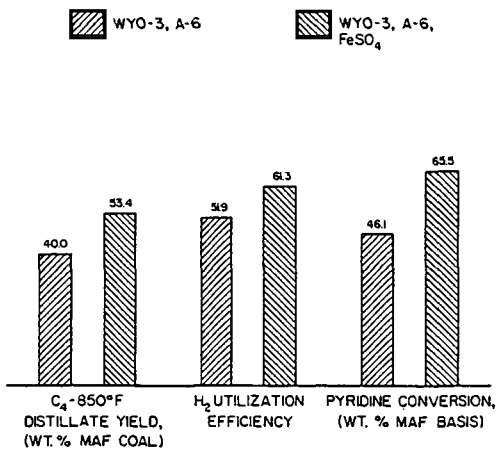


Figure 6. Liquefaction Co-Processing Yield Results using Carbon Monoxide/Water (Reaction Conditions: 600°F, 1500 psig CO, 30 min.)

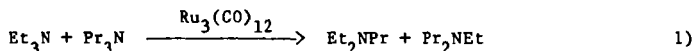
## NEW CATALYSTS FOR HYDROTREATING COAL LIQUIDS

A. S. Hirschon, R. B. Wilson, Jr. and R. M. Laine\*

SRI International, Menlo Park, CA 94025

The cost of hydrotreating coal liquids or heavy crudes is considerably higher than for light crudes because of the significantly higher amounts of sulfur, nitrogen and oxygen found in these hydrocarbon sources relative to light crudes. In particular, the current processes for the catalytic removal of nitrogen (HDN) and oxygen (HDO) consume excessive amounts of hydrogen due to concurrent hydrogenation of aromatics. The ideal HDN or HDO catalyst would be one that selectively cleaves C-N or C-O bonds with minimum consumption of hydrogen. This would reduce the overall hydrotreating costs for refining crude oil and could make synfuels a competitive energy source.

In this paper, we discuss the results of two approaches to the development of improved HDN catalysts. One approach focuses on the synthesis of high-activity, highly dispersed, "surface confined", catalysts using organometallic complexes. The other approach examines the hydrotreating activities of metals not currently used in HDN and HDO catalysis. This latter investigation arises as a consequence of our efforts to develop mechanistic models of HDN through studies of the homogeneous catalysis of the transalkylation reaction, (1,2) equation 1,



and through studies of quinoline HDN by bulk metals (3). In both the trans-alkylation and the bulk metal studies; ruthenium exhibits the highest activity for C-N bond cleavage. This suggests that it may be useful as an HDN catalyst.

We describe here the synthesis and HDN activities of catalysts prepared according to the principles established by these two separate approaches.

### Experimental

#### Materials

The CoMo catalyst (HT-400, 3 wt% CoO, 15.1 wt% MoO<sub>3</sub>, on Al<sub>2</sub>O<sub>3</sub>) was donated by Harshaw Chemical Company. The preparation of the sulfided catalyst has been described previously.<sup>4</sup>  $\gamma$ -aluminum oxide was donated by Kaiser Aluminum and was made from Gibbsite (surface area = 210 m<sup>2</sup>/g and passed 400 mesh sieve.) The aluminum oxide was calcined at 400°C for 2h under flowing synthetic air. Ruthenium was obtained from Strem Chemical, and was heated at 400°C for 12 h first with flowing synthetic air to remove any surface sulfur, and then with flowing hydrogen to form the reduced metal. Ruthenium carbonyl [Ru<sub>3</sub>(CO)<sub>12</sub>] and nickel cyclooctadiene [Ni(COD)<sub>2</sub>] were obtained from Strem Chemicals and used as received. Molybdenum(II) allyl dimer was prepared by modifying the method of Cotton and Pipal (5).

#### Preparation of a Conventional NiMo Catalyst

Ammonium molybdate tetrahydrate (2.10 g, 1.7 mol) and nickel nitrate hexahydrate (1.34 g, 4.6 mmol) were dissolved in 200 mL of water. Alumina, 10 g, was added to the metal salt solution and stirred for 24 h. The water was evaporated from the mixture, and the residue was slowly heated to 400 C under flowing synthetic air over a 2-h period. The heating was continued for 12 h. The process was repeated for another 12 h with flowing H<sub>2</sub>S (10%)/H<sub>2</sub>.

### Preparation of Supported Organometallic Catalysts

Molybdenum Supported on Alumina. Molybdenum allyl dimer (1.0 g) dissolved in 10 mL of hexane was slowly added to a stirred slurry of 10 g of alumina in 20 mL of hexane. The mixture was stirred overnight, then washed with 20 mL of hexane to give a gray solid. The product was then heated at 200 C in flowing  $H_2S(10\%)/H_2$  for 12 h.

Bimetallic Metal Supported Catalysts. An aliquot (1 g) of the sulfided supported molybdenum catalyst was suspended in 10 mL of hexane. The desired amount of Ni (as  $Ni(COD)_2$ ) in THF was added to the suspension and the mixture stirred overnight, washed with hexane, dried, and sulfided at 200 C as described above.

Ruthenium doped CoMo Catalyst (RuCoMo). Under nitrogen, ruthenium carbonyl (0.053 g), dissolved in 5 mL of hexane, was added to a stirred slurry of 2.00 g of the sulfided CoMo catalyst in 10 mL of hexane. The mixture was allowed to stir for 72 h. The hexane was then evaporated and the residue heated under vacuum at 76°C for 6 h. A portion of the doped catalyst was sulfided by treating with a flowing mixture of  $H_2S(10\%)/H_2$  at 200°C for 12 h.

### Standard HDN Reaction Procedures

The following materials were placed in a quartz liner, under nitrogen in a 45-mL Parr bomb: the catalyst (0.100 to .250 g), a stirbar, and 10 mL of 0.197 M quinoline (0.151 M THQ for Ru reactions) and 0.098 M n-dodecane (as internal standard) in n-hexadecane. The bomb was pressurized with 500 psia of  $H_2$ , and heated at the desired temperature.

### Results and Discussion

The HDN activities of the catalysts prepared by the various synthetic techniques were compared using a quinoline/hexadecane solution for model studies. As shown in Figure 1, quinoline HDN leads to two major HDN products; propylcyclohexane (PCH) and propylbenzene (PB). In comparing the catalytic properties of the various catalysts, we use two criteria, rate of HDN and, as discussed above, hydrogen consumption. The production of PCH requires 7 moles of  $H_2$  per quinoline and typifies aromatic hydrogenation, whereas the production of PB requires only 3 moles; thus the relative ratios of PCH to PB are an excellent measure of hydrogen consumption.

### Comparison of Conventional NiMo and Organometallic Origin NiMo Catalysts

Table 1 lists the estimated turnover frequencies (TF = moles THQ reacted/mole of metal catalyst/hour  $\pm$  10%) for THQ disappearance, and the appearance of PCH, PCHE, and PB, calculated based on initial rates. From this data we see that the organometallic origin or surface confined NiMo catalysts exhibit higher hydrogenation activity than a conventionally prepared NiMo catalyst. In a similar manner and from Figures 2a-c, it can be seen that the surface confined catalysts are superior in terms of C-N bond cleavage activity.

The total metal content in the catalysts is approximately the same, so that the activity and selectivity of these catalysts can qualitatively be compared. Figure 3 presents calculations of the total hydrocarbon conversion as a sum of PCH, PB and propylcyclohexene (PCHE) as a function of time.

To compare the relative PCH, PCHE and PB selectivities for the various catalysts, the relative distributions of these products, normalized to 5% total hydrocarbon conversion, were extracted from Figure 3 and are listed in Table 2. We see, in Table 2, that the product selectivities for the NiMo catalyst of organo-

metallic origin (surface confined catalyst) are essentially the same as those found with the conventionally prepared NiMo catalyst.

Table 1  
TURNOVER FREQUENCIES<sup>a</sup>

Catalyst	THQ	PCH	PB	PCHE
NiMo (conventional)	67.4	8.2	0.3	1.4
NiMo (0.83, 2.63)	111	26.5	1.4	--
NiMo (0.37, 2.81)	104	16.6	0.7	1.7
CoMo	54.0	8.9	0.5	0.8
RuCoMo	141	26.9	8.0	0

<sup>a</sup>Moles product/moles metal catalyst/h.

Table 2  
HYDROCARBON DISTRIBUTION AT 5 mol%  
HDN CONVERSION<sup>a</sup>

Catalyst	%PCH	%PB	%PCHE
NiMo (conventional)	76.2	5.2	18.6
NiMo (0.37% Ni, 2.81% Mo)	81.4	3.1	15.5
NiMo (0.83% Ni, 2.63% Mo)	76.0	5.0	19.0
CoMo	82.2	4.6	13.2
RuCoMo	76.6	23.4	0

<sup>a</sup>Reaction of 10 mL 0.197 M quinoline in n-hexadecane and catalyst at 350°C and 500 psig H<sub>2</sub>.

#### Bulk Ruthenium HDN Catalysis

Figure 4 shows the product distribution from the reaction of bulk ruthenium with THQ at 200, 250 and 300°C. These results demonstrate ruthenium's high activity for C-N bond cleavage even at temperatures of 200°C. At 200 and 250°C the major HDN products are propyl- or ethyl- and methyl-cyclohexylamine, but at 300°C almost no nitrogen containing species remain after 3 hours of reaction time due to extensive

C-N and C-C bond hydrogenolysis. If the bulk ruthenium is exposed to sulfur in the form of CS<sub>2</sub> (20 µl to the standard reaction), then even at temperatures up to 350°C, no reaction of any type is observed. Thus, sulfur poisons bulk ruthenium's ability to catalyze both hydrogenation and C-N bond cleavage.

#### Ruthenium-Doped Harshaw CoMo Catalysts

In an attempt to overcome the difficulty of sulfur poisoning with the ruthenium, we doped a commercial CoMo catalyst with a ruthenium containing organometallic. Figure 5a and b show the product distribution after reaction with a sulfided Harshaw CoMo catalyst and the same catalyst doped with ruthenium. As seen in these figures, the doped catalyst is significantly more active, produces no PCHE, and gives a much higher ratio of propylbenzene to propylcyclohexane than does the "unpromoted" CoMo catalyst. As shown in Figure 3, the total hydrocarbon production is greater for the ruthenium-"promoted" catalyst than any of the other catalysts studied. This catalyst, as shown in Table 2, also produces the most propylbenzene of any of the catalysts studied. For instance, after 5% conversion, the fraction of propylbenzene in the hydrocarbon products has increased from 4.6% for the CoMo catalyst to 23.4% for the RuCoMo catalyst. Furthermore, when this catalyst was treated with carbon disulfide, as was the bulk ruthenium, the catalyst was even more active towards HDN activity.

#### Conclusions

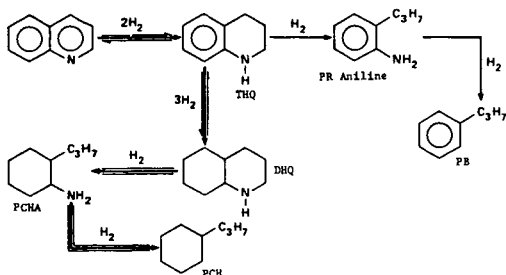
We have shown that the activity of HDN catalysts using conventional metals, such as nickel and molybdenum can be improved using organometallic precursors; although, in our hands, the selectivity of aromatic and aliphatic hydrocarbon products remained unchanged from that of conventional based catalysts. However, through the use of more active metals such as ruthenium, we can promote a conventional type catalyst to give a catalyst which is not only more active, but is more selective towards aromatic products, and remains sulfur tolerant.

#### Acknowledgements:

We would like to thank the Department of Energy, Pittsburgh Energy and Technology Center for support of this work through grants DE-FG22-83PC60781 and DE-FG-85PC80906. We would also like to thank NSF for partial support of this work through grant CHE 82-19541.

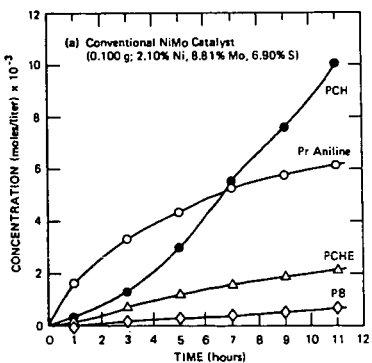
#### References

1. R. B. Wilson Jr. and R. M. Laine, J. Am. Chem. Soc. (1985) 107, 361-369.
2. R. M. Laine, D. W. Thomas, L. W. Cary, J. Am. Chem. Soc. (1982) 104, 1763.
3. A. S. Hirschon and R. M. Laine, manuscript in preparation.
4. A. S. Hirschon and R. M. Laine, Fuel (1985) 64, 868-870.



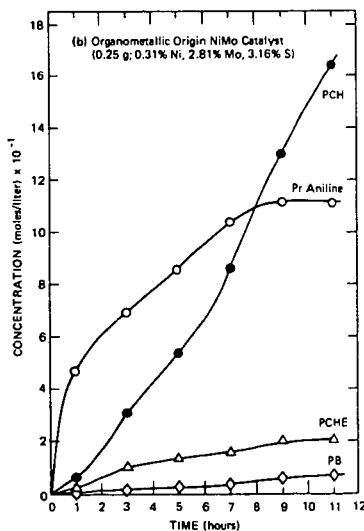
JA-6762-1

FIGURE 1 QUINOLINE HDN REACTION NETWORK



JA-6762-18A

FIGURE 2a PRODUCT DISTRIBUTION DUE TO CARBON-NITROGEN CLEAVAGE REACTIONS  
10 mL of 0.197 M quinoline in *n*-hexadecane and sulfided NiMo catalyst at 350°C and 500 psia H<sub>2</sub>.



JA-6762-27A

FIGURE 2b PRODUCT DISTRIBUTION DUE TO CARBON-NITROGEN CLEAVAGE REACTIONS (Continued)  
10 mL of 0.197 M quinoline in *n*-hexadecane and sulfided NiMo catalyst at 350°C and 500 psia H<sub>2</sub>.

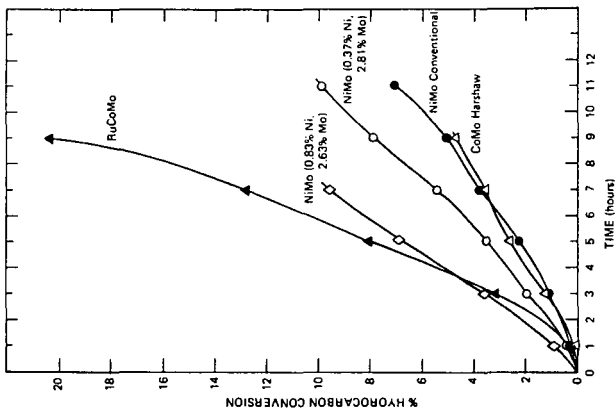


FIGURE 3 TOTAL HYDROCARBON CONVERSION  
JA-4882-16

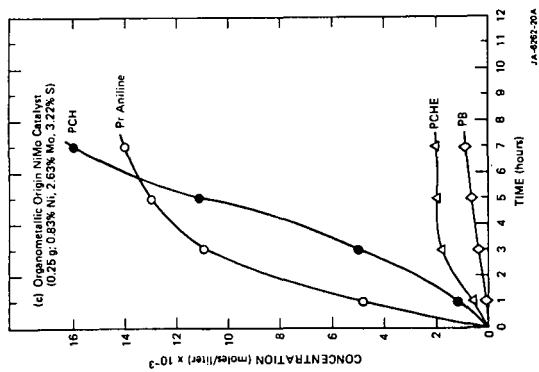
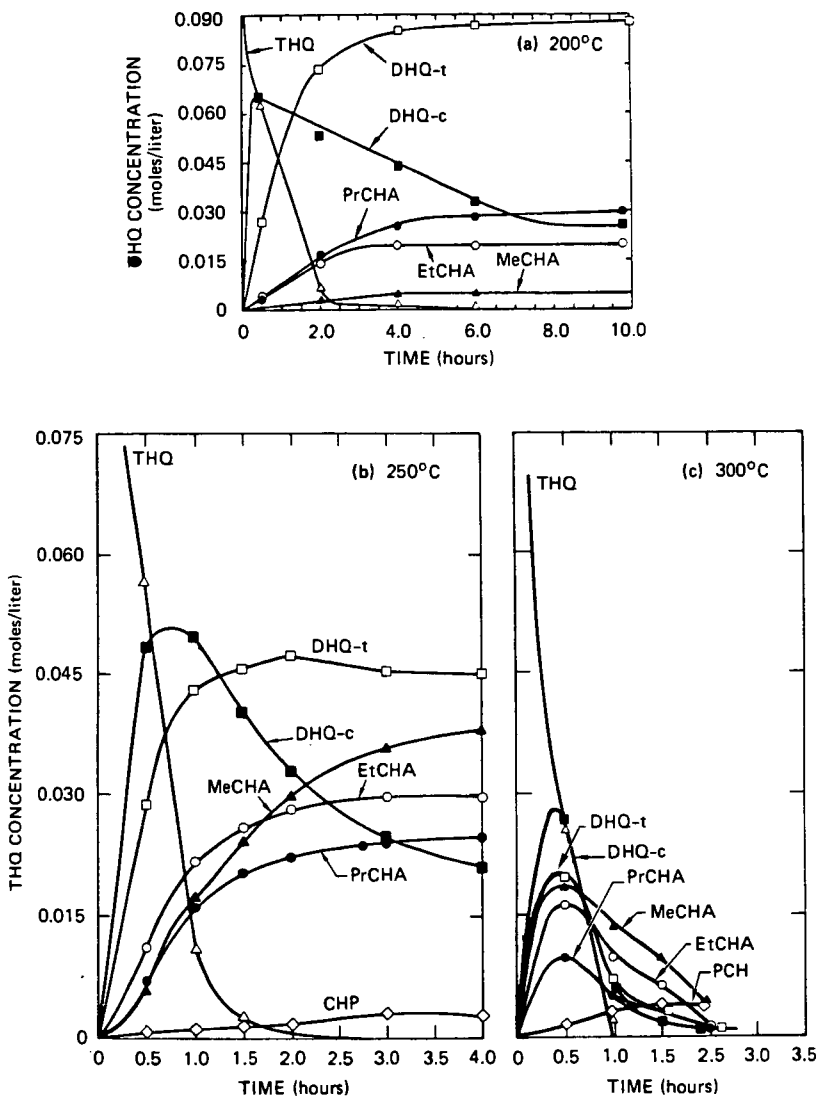


FIGURE 2c PRODUCT DISTRIBUTION DUE TO CARBON-NITROGEN  
CLEAVAGE REACTIONS (Continued)  
10 mL of 0.197 M quinoline in n-hexadecane and sulfided NiMo catalyst  
at 350°C and 500 psia H<sub>2</sub>.  
JA-4882-20A



JA-6262-9A

FIGURE 4 PRODUCT DISTRIBUTION FROM REACTION OF THQ WITH RUTHENIUM AND 500 psi of  $H_2$   
 10 mL of 0.1506 M THQ and 0.100 g of Ru in hexadecane.  
 316

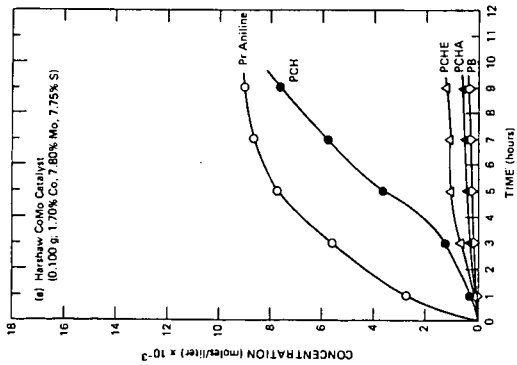


FIGURE 3a PRODUCT DISTRIBUTION DUE TO CARBON-NITROGEN CLEAVAGE REACTIONS WITH CoMo CATALYST (10 mL of 0.197 g/liter *m*-hexanamine and sulfided CoMo catalyst at 350°C and 500 psia H<sub>2</sub>).

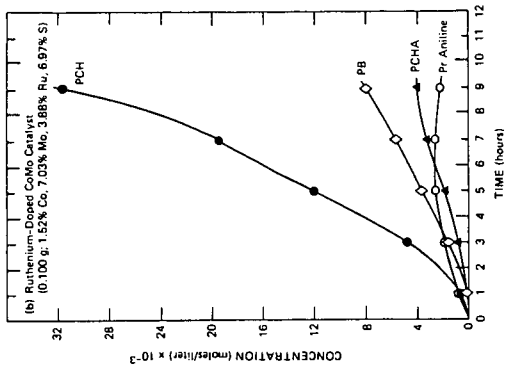


FIGURE 3b PRODUCT DISTRIBUTION DUE TO CARBON-NITROGEN CLEAVAGE REACTIONS WITH CoMo CATALYST (10 mL of 0.197 g/liter *m*-hexanamine and Ru-CoMo catalyst at 350°C and 500 psia H<sub>2</sub>).

## FTIR SPECTROSCOPIC STUDIES OF COAL LIQUEFACTION PRODUCTS

Jack Youtcheff, Paul Painter and Peter Given

Mineral Industries Research Lab  
University of Alaska  
Fairbanks, Alaska 99701

AND

Materials Science Department  
The Pennsylvania State University  
University Park, PA 16802

Recent work in our laboratories has been concerned with obtaining a better understanding of the phenomena associated with coal liquefaction (1). An initial study of three bituminous coals discussed the changes that occur in oxygen containing functional groups (2). It was concluded that the initial large loss of so-called "unaccounted" oxygen was a result of a cleavage of ether groups to form hydroxyls, which were subsequently removed by dehydroxylation. These same samples were also characterized by FTIR and the results of this portion of the work are presented in this communication.

As might be expected, the most interesting changes occurred in the aliphatic and aromatic CH stretching regions of the spectrum. Samples were prepared for infrared analysis using established KBr pellet techniques (1,3) and representative spectra of the three coals, PSOC 521 (HVC), PSOC 767 (HVB) and PSOC 757 (HVA) are presented in figure 1. Even though the aromatic CH stretching modes between 3100 and 3000  $\text{cm}^{-1}$  are relatively weak, it can be seen that there is still a degree of overlap that can lead to errors when band areas are determined by simple integration. Accordingly, a curve resolving procedure, described in previous publications (1,3), was used to separate the two contributions. In addition, it was found that there was a change in the relative proportion of various aliphatic CH groups. In order to sort this out second derivative methods were used to define the initial positions of five bands that were curve-fit to the difference spectrum obtained by subtracting the aromatic CH stretching modes, as illustrated in figure 2. These bands do not represent individual components, but are themselves composites (4). Nevertheless, the bands near 2956 and 2867  $\text{cm}^{-1}$  are largely due to methyl groups, the bands near 2923 and 2852  $\text{cm}^{-1}$  have a major contribution from methylene groups, while the band at 2893  $\text{cm}^{-1}$  can be assigned to methine CH moieties.

Liquefaction reactions were carried out at temperatures of 350, 370, 400 and 425°C for periods of 2, 12, 22 and 32 minutes, as described previously (1,2). Overall, the spectra of the liquefaction products from a particular coal were surprisingly similar, supporting the notion that structural rearrangement under these reaction conditions is relatively limited. The integrated area of the aromatic CH stretching modes increases with the severity of the liquefaction conditions, but it should be kept in mind that to some extent this is an apparent increase that is due to the loss of oxygen containing functional groups. The pattern of out-of-plane bending modes between 900 and 700  $\text{cm}^{-1}$  shows little change in the distribution pattern of hydrogen in aromatic units, supporting the inference that the changes in this region are largely due to the loss of other groups and hence an increase in the per unit weight concentrations of those left behind.

Although this factor also affects the aliphatic CH stretching modes, the changes in this region are far more pronounced. The overall aliphatic CH content appears to initially increase with conversion, but then drops off somewhat

at conditions of high conversion. The data, however, shows considerable scatter and such conclusions are only tentative. There are much clearer changes in individual curve-resolved bands, (measured as a fraction of total aliphatic CH area, in order to eliminate and reduce errors in sample preparation, etc.), with the most marked differences being observed in the  $2956\text{ cm}^{-1}$  band. The relative area of this band is plotted as a function of reaction time and conversion in figures 3 and 4, respectively.

The Ohio coal (PSOC 757) showed no temperature dependence in the plot against time, in contrast to the other coals. When the  $2956\text{ cm}^{-1}$  band is plotted as a function of conversion (figure 4), the points for all temperatures tend to lie in a single band. Visual inspection suggests that the band or line is somewhat curved. However, linear regressions were performed and gave surprisingly high variance, particularly for the Oklahoma and Wyoming coals. Nevertheless, the slopes of these least-squares fits suggest that the number or type of bonds broken during liquefaction are different for the three coals. For a slope of zero to exist in figure 4, the distribution of aliphatics in the parent coal and products would have to be the same. This would result if no chemical reactions were involved, and conversion results from the physical dissolution of the coal. An increase in this slope is indicative of an increasing number of alkyl ethers or aliphatic systems cleaved in converting a particular coal. If the increase in relative area of this band stems from methyl-generating reactions, for the Ohio coal (PSOC 757), only a few bonds need to be broken to drastically enhance its conversion.

In figure 5, the amount of "ethers" cleaved (loss of unaccounted oxygen from references 1 and 2) is plotted against the area of the  $2956\text{ cm}^{-1}$  band as a fraction of the total area for aliphatic C-H stretching vibrations. Correlations are readily apparent for the coals having a higher number of cleavable ethers, namely the Wyoming and Ohio coals with 7.7 and 5.1 cleavable ethers per 100 carbon atoms, respectively. A least-squares linear regression was performed on the values at the three lowest temperatures for the Wyoming coal (Figure 5 (b)). The slopes and the  $R^2$  values for this correlation between ether removal and relative area of the  $2956\text{ cm}^{-1}$  band show a high proportion of variance explained. If the correlation is accepted, the obvious inference is that ether cleavages generate methyl groups (i.e.  $-O-CH_2-$  bonds are cleaved forming OH and  $CH_3$ ). It should be noted that the slopes of the least-squares fit for the lowest three temperatures are quite similar, whereas the curves for the Ohio coal (figure 5 (c)) increase more steeply with increasing temperature. For the latter case, one could infer that at the lower temperatures, labile ethers (aliphatic and benzylic) are cleaved; proceeding to higher temperatures, the more refractory type of ethers (diaryl) are likely to be cleaved. The fact that the slopes are similar for the Wyoming coal suggests that similar types of ethers are broken under these conditions. The relatively small slopes suggest that these ethers are predominantly aliphatic or aralkyl. The lack of correlation at  $425^\circ\text{C}$  for this coal and the poor correlation at all temperatures for the Oklahoma coal (though a trend similar to that of the Ohio coal exists) arises perhaps because any trend is marked by alkyl cleavage and other reactions that do not involve loss of unaccounted oxygen.

In conclusion, the FTIR results indicate that extensive structural rearrangements are not occurring during liquefaction. Rather, a few selected bridging units are broken, resulting in the formation of various fragments of different solubility. The increase in methyl groups and previously reported loss of ether oxygen indicates

that bonds between aliphatic methylene units, benzylic ethers and aryl alkyl ethers are the principal sites of cleavage.

#### References

1. Youtcheff, J. S. and Given, P. H. "The dependence of liquefaction behavior on coal characteristics" and references therein. Final Report to DOE under Contract No DE-AC22-81-PC-40784, September 1983.
2. Youtcheff, J. S. and Given, P. H. *Fuel*, 61, 980 (1982).
3. Sobkowiak, M., Reisser, E., Given, P. and Painter, P. *Fuel*, 63, 1245 (1984).
4. Painter, P. C., Starsinic, M. and Coleman, M. M. in "Fourier Transform Infrared Spectroscopy", Vol 4. (edited by J. R. Ferraro and L. J. Basile) pp 169-243 Academic Press (1985).

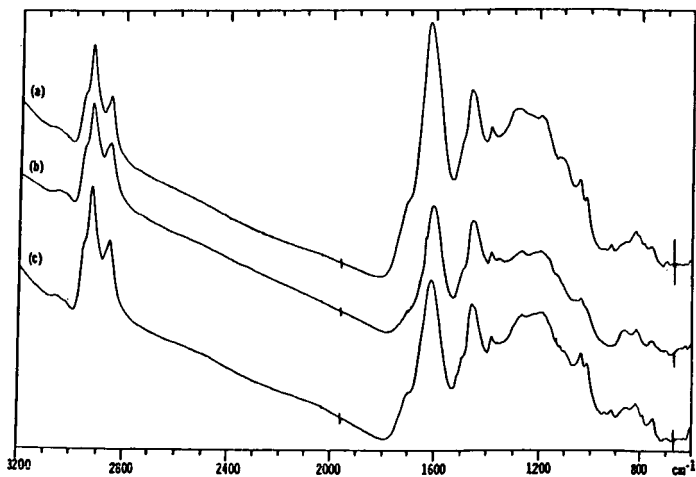


Figure 1. FTIR SPECTRA OF COALS (a) PSOC-521; (b) PSOC-767; (c) PSOC-757

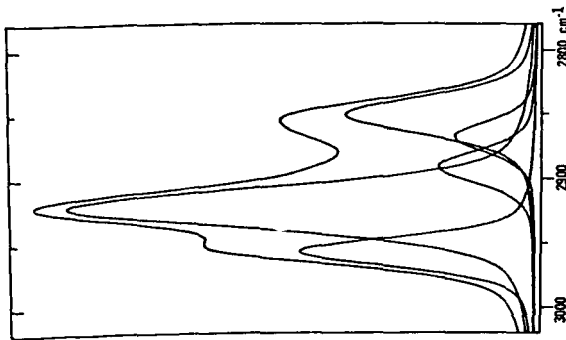


Figure 2. RESOLUTION OF THE DIFFERENCE SPECTRUM OF THE ALIPHATIC C-H STRETCH REGION INTO INDIVIDUAL BANDS (envelope synthesized by co-adding individual bands is superimposed)

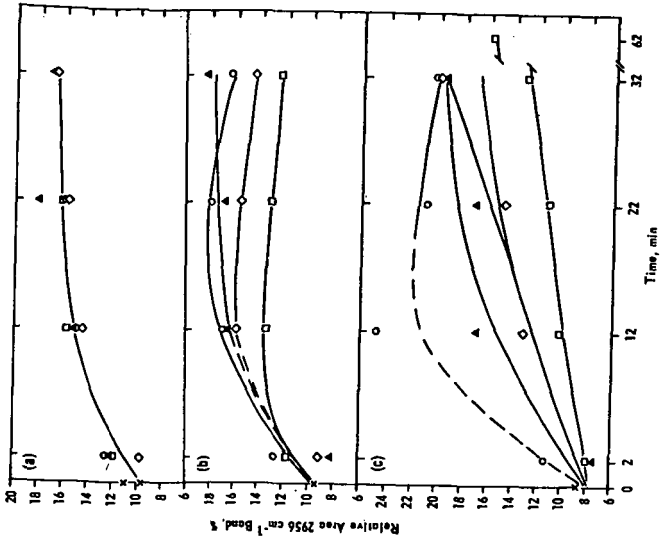


Figure 3. CHANGE IN RELATIVE AREA OF 2956  $\text{cm}^{-1}$  BAND FOR COAL AS A FUNCTION OF TIME (a) PSOC-757; (b) PSOC-767 (c) PSOC-521  
 o 425°C 400°C 370°C 350°C

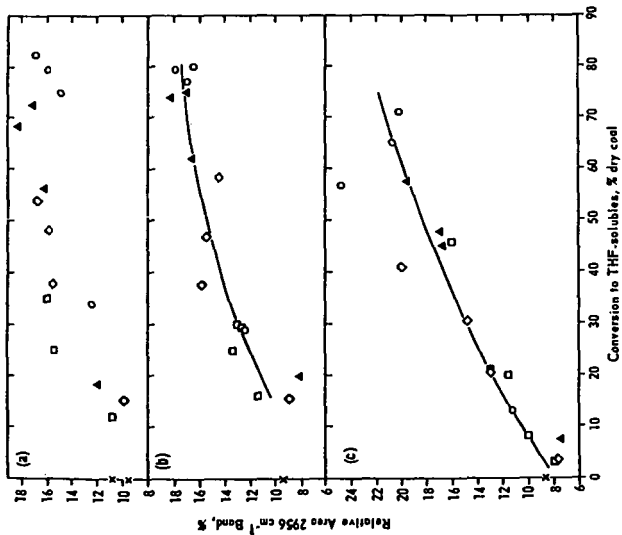


Figure 4. CHANGE IN RELATIVE AREA OF 2956  $\text{cm}^{-1}$  BAND FOR COALS AS A FUNCTION OF CONVERSION TO THF-solubles, % dry coal  
 (a) PSOC-757; (b) PSOC-767 (c) PSOC-521  
 o 425°C 400°C 370°C 350°C

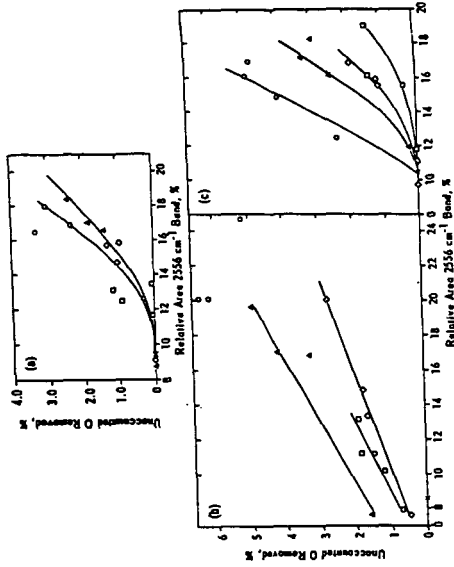


Figure 5. RELATION OF UNACCOUNTED  $\text{O}_1$  REMOVED TO THE RELATIVE AREA OF 2956  $\text{cm}^{-1}$  BAND  
 (a) PSOC-767; (b) PSOC-521; (c) PSOC-757  
 o 425°C 400°C 370°C 350°C

## PHYSICAL BENEFICIATION OF CHAR AND CHEMICALLY CONDITIONED COAL

Robert P. Warzinski and Joseph A. Cavallaro

U.S. Department of Energy  
Pittsburgh Energy Technology Center  
Pittsburgh, Pennsylvania 15236.

### ABSTRACT

Demineralization of coals and coal-derived chars is part of an effort to develop alternative fuels from coal. Pyrolysis and some gasification processes yield chars containing a large fraction of the calorific value of the feed coal and essentially all of its mineral matter. In the work reported here, three gasification chars produced from anthracite, bituminous, and subbituminous coals have been subjected to specific gravity separation to determine their yield-ash relationships. Either low yields or high ash levels in the float products were observed. Also reported is preliminary work concerning the use of chemical conditioning to enhance the cleanability of coal prior to physical beneficiation. Conditioning of an Illinois No. 6 River King Mine coal with either supercritical methanol or cyclohexane resulted in an improved yield-ash relationship, whereas similar treatment with supercritical toluene had a negative effect.

### INTRODUCTION

Currently, there is increasing interest in the identification, development, and characterization of new coal-derived fuels which have application extending beyond traditional electric utility markets into the commercial, industrial, residential, and transportation sectors of our economy. To penetrate these markets, new fuels must be low in both total sulfur and mineral matter. Emphasis is therefore being placed on the development of new processes to provide ultraclean coal having less than one percent mineral matter. In one recent example coal is subjected to physical beneficiation, pyrolysis, and subsequent beneficiation of the char [1]. In this scheme, a portion of the char is combined with the pyrolysis liquids to produce a heavy oil substitute. In order for the process to be profitable, however, the excess char must be sold at a premium price, such as in the residential heating market.

Results from two different areas of research concerned with the development of alternative fuels from coal will be presented in this paper. The first area involves beneficiation of chars produced from coal. Such chars may be a major product of gasification and pyrolysis processes used to produce premium liquid and gaseous fuels. Since a large portion of the calorific value often ends up in the char, the beneficiation of this material to produce a premium fuel can be important from a process economics standpoint.

The second area of research is concerned with the use of a chemical pretreatment to improve mineral matter liberation during subsequent physical beneficiation. Advantages of this reversal of the conventional order of treatment have been discussed elsewhere [2]. Reported here are preliminary results from the use of supercritical fluids in the initial chemical-pretreatment step.

For reasons of clarity, the following discussion of methodology and results is divided into two parts. The first section describes the beneficiation of the gasification chars, and the second the work on conditioning of coal prior to its physical beneficiation. After this, an overall conclusion section summarizes both areas of research.

## I. BENEFICIATION OF GASIFICATION CHARs

### EXPERIMENTAL

Three gasification chars produced at the Pittsburgh Energy Technology Center were used for the beneficiation tests. These chars were formed from three different coals: a Pennsylvania anthracite coal, a Pittsburgh seam bituminous coal from the Bruceston Experimental Research Mine, and a Montana subbituminous coal from the Rosebud Mine. These coals were gasified at approximately 1160 K under a combined oxygen/steam pressure of 4.1 MPa in the Synthane Process Development Unit (PDU) gasification system. The PDU system combined the steps of fluidized-bed pre-treatment, free-fall carbonization, and fluidized-bed gasification [3]. Table 1 contains the analysis of the three chars used.

Beneficiation of the gasification chars involved a washability determination on the char as received and after additional crushing. A high-speed centrifuge equipped with four 0.5 L hourglass-shaped flasks was used to effect the specific gravity separations. Enough heavy organic liquid was added to fill each centrifuge flask just above the neck. The specific gravity was checked with a spindle hydrometer to within  $\pm 0.001$  of a specific gravity unit.

Four 25-gram samples were riffled from each char using a microsplitter. The 25-gram char samples were then added to the flasks along with enough additional liquid to bring the liquid level to within 1.5 cm of the top of the flask. The samples were centrifuged for 20 minutes at 1500 rpm, and the centrifuge was allowed to stop without braking. After removing the flasks, thin rubber inserts were put in the necks, and the float products were carefully poured off. The rubber inserts were removed to recover the sink products. Both products were vacuum filtered to remove the heavy liquid, air dried, and weighed.

The total sink product was divided into two or four equal portions by weight and then added to the centrifuge flasks containing the next higher specific gravity liquid. This procedure was repeated for each specific gravity. Each product was analyzed for calorific value, ash, and total sulfur. All results are tabulated as cumulative values and are reported on a moisture-free basis.

Another riffled portion of each char sample was crushed to either 200- or 325-mesh top size, and similar tests and analyses were performed to determine the effects of crushing on the liberation of ash and its subsequent removal.

### DISCUSSION OF RESULTS

The results of the specific gravity separations for the three as-received and crushed chars are contained in Tables 2, 3, and 4. For the anthracite coal gasification char shown in Table 2, the as-received sample contained 69.7 wt% plus-200-mesh material. After crushing, 91.9 wt% of the sample was minus-325 mesh. For the as-received sample, 79.1 wt% could be recovered at 2.00 specific gravity, analyzing 7.6 wt% ash. This represents a 54% ash reduction. After crushing, only 44.0 wt% was recovered at the same specific gravity, and only a 10% ash reduction was observed.

The data for the bituminous coal gasification char are contained in Table 3. Initially 76.5 wt% of the char was plus-200 mesh. After crushing, all of the sample was minus-200 mesh. At a specific gravity of 1.80, 87 wt% of the char was recovered; however the ash reduction was only 28%. After crushing, the ash content of the float 1.80 specific gravity product was only 4.1 wt%, but the weight recovery was only 20.5%.

Table 4 contains the results for the subbituminous coal gasification char. The as-received char contained 44.7 wt% plus-200-mesh material. After crushing,

96.8 wt% was minus-200 mesh. The float-sink tests show a 72% ash reduction for the as-received material recovered at 1.80 specific gravity. However, as with the bituminous coal, the weight recovery is quite low. For this char, crushing appears to be of no benefit, as the yield/ash relationship for the crushed char is essentially the same as for the as-received material.

It is apparent from these washability data that the apparent particle density of the chars is higher than that observed for coal. In most of the tests, less than 20 wt% of the char would float in liquids of 1.80 specific gravity. For most raw coals, upwards of 70 wt% would float in such liquids, with only the concentrated mineral matter occurring in the sink product. Also, for coal, crushing to a finer size typically improves the yield/ash relationship. For the chars, crushing was either of no value or resulted in a poorer yield/ash relationship.

To explain these observations, phenomena occurring during the formation of the chars must be considered. Under the high-temperature gasification conditions, the pore structure of the coal may collapse or otherwise be destroyed; and as a result, a denser form of carbon would exist in the char. Also under these conditions, the volatile matter is driven off. Loss of this relatively light material would also cause an increase in the apparent particle density. Finally, encapsulation of the mineral matter by the organic phase would increase the apparent particle density and also result in a more homogeneous material that would be difficult to beneficiate by physical means. Encapsulation of the ash would also explain why these gasification chars were less responsive to grinding for release of mineral matter than typical coals, since there would be less segregation of the various materials. We have visually observed under the microscope such encapsulation of the ash in other chars produced by similar high-temperature processing.

## II. CONDITIONING OF COAL PRIOR TO PHYSICAL BENEFICIATION

### EXPERIMENTAL

A unit has been designed and constructed to process coal and coal-derived materials with supercritical fluids. Figure 1 contains a sectional view of the heart of this apparatus, the supercritical fluid extraction vessel. The vessel is constructed entirely of 316 stainless steel and can be operated at conditions up to 673 K at 27.6 MPa. In the work reported here, the reflux column, which consists of a packed bed and condenser section, was maintained at the same temperature as the extraction section. The use of a temperature difference across the column to exploit the properties of supercritical fluids to fractionate non-distillable coal-derived liquids has been reported elsewhere [4].

The coal used in this work was a channel sample of Illinois No. 6 coal from the River King Mine containing 8.31 percent moisture, 13.33 percent ash, and 4.68 percent sulfur. Supercritical methanol ( $T_c = 512.6$  K;  $P_c = 8.097$  MPa), cyclohexane ( $T_c = 553.4$  K;  $P_c = 4.074$  MPa), and toluene ( $T_c = 591.7$  K;  $P_c = 4.115$  MPa) were used in the treatment of this coal. The solvents were obtained in drum quantities at greater than 99 percent purity and used as received.

A 500-gram charge of the coal, crushed to minus-14 mesh, is first placed in the extraction section of the supercritical fluid extraction vessel. After the unit is stabilized at operating conditions under a nitrogen atmosphere, the supercritical fluid is introduced into the bottom of the vessel through the sparger, where it contacts the coal. The fluid phase containing extracted material continues up the column and exits at the top of the vessel. The extracted material leaving the column is separated from the supercritical fluid by partial depressurization. The fluid is then condensed for reuse. Before being recycled in the unit, the solvents are distilled on a rotary evaporator.

The Illinois No. 6 coal was processed with methanol, cyclohexane, and toluene at a  $T_r$ , or  $T/T_C$ , of 1.02, and at a  $P_r$ , or  $P/P_C$ , of 2.0. The runs were terminated when the rate of collection of extracted material was less than 1 gram in 30 minutes. This required from 5 to 9 hours of operation. The flow of solvent was maintained at 0.27 gram-moles/minute during most of this work. This rate was doubled in one of the toluene treatments. No appreciable change was observed in the yield of extract in this case. To provide sufficient material for characterization and physical beneficiation testing, two runs were made with each solvent, and the respective products were combined. The yields of treated coal on a moisture-free basis were 90, 89, and 75 weight percent for methanol, cyclohexane, and toluene, respectively. The overall material balance, defined as the total weight of recovered material divided by the weight of the coal initially charged, ranged from 95 to 102 percent for all the tests.

Specific gravity separations of the treated coals were performed using conventional static float-sink techniques to determine their beneficiation potential.

#### DISCUSSION OF RESULTS

Tables 5 through 8 contain the results from the washability analysis of the Illinois No. 6 coal before and after treatment. These data are cumulative values and are reported on a moisture-free basis. Also shown in these tables are ash, total sulfur, and calorific value data obtained on the bulk samples prior to the specific gravity separations. The agreement between the bulk values and the results reconstituted from the washability data is generally acceptable. Noteworthy exceptions are the total sulfur contents of the coals treated with methanol and cyclohexane and the ash content of the toluene-treated coal. Additional work is being performed to find an explanation for these differences.

Reduction in total sulfur concentration is only observed in the specific gravity separation products of the methanol-treated coal. The higher total sulfur levels resulting from the cyclohexane and toluene treatments are primarily due to the extraction of a portion of the organic phase, which concentrates the remaining sulfur in the treated coal. The extractable materials from all of the tests contain approximately 2.4 wt% sulfur and no mineral matter. Sulfur balances for the treated coals using the bulk sample sulfur data are between 95 and 99 percent.

Unusually low levels of pyritic sulfur are reported for the cyclohexane-treated coal. The total sulfur, however, did not decrease by a corresponding amount, indicating either that organic sulfur was formed from the sulfur originally contained in the pyrite or that the analysis for pyritic sulfur is in error. Under the relatively mild reaction conditions, it is not likely that sulfur from the pyrite has incorporated into the organic matrix of the coal. Rather, the pyrite has probably been transformed into a form that does not dissolve in the acid used for the pyritic sulfur determination.

In contrast to the other treated coals, the total and pyritic sulfur levels in the toluene-treated coal remain high, even in the low specific gravity fractions. One possible explanation is that the toluene treatment caused a softening of the organic portion of the coal, resulting in increased encapsulation of the mineral matter. This would make the material more homogeneous with respect to the specific gravity separations. Softening of the coal was evidenced by the fact that the coal was mildly agglomerated after the toluene treatment. After treatment with either methanol or cyclohexane, however, the product was free-flowing and similar in appearance to the starting material.

Microscopic analysis of the various specific gravity fractions shows the toluene treatment produces particles that contain relatively more and larger pore openings than the particles after methanol or cyclohexane treatment. This characteristic could decrease the apparent specific gravities of the coal particles and result in

the poor sulfur rejection observed for the toluene-treated coal. This phenomenon would explain the high yield in the Float-1.25 fraction. Several other coals have been treated to provide a larger frame of reference from which to investigate these observations.

In order to illustrate the changes in the true and/or apparent specific gravities of the coal particles resulting from the supercritical fluid treatments, the yield versus ash content data are plotted in Figure 2 for the raw and treated coals. In comparison with raw coal washability data, both the methanol and cyclohexane treatments marginally enhance the cleanability of the raw coal. In contrast, the toluene treatment makes it worse. Additional work with other solvents is in progress to determine if the positive trends observed with methanol and cyclohexane can be improved.

#### CONCLUSIONS

A set of three gasification chars have been subjected to physical beneficiation. In some cases, marginal improvements in the mineral matter content were achieved, but either unsatisfactory ash liberation or low yields were observed overall. The form of carbon in the ash is much denser than that typical for coal. One explanation for this observation is that some of the mineral matter has been encapsulated during the formation of the char. This is further evidenced by the poor response of the chars upon further size reduction. Other phenomena, such as loss of porosity and volatile matter, may also contribute to the poor separations observed. In summary, these observations highlight the inadequacy of conventional physical-cleaning methods for some coal-derived materials. If a clean char product is to be produced, either deeper initial cleaning of the coal is required or new techniques must be developed to separate the mineral matter from the resulting chars.

The washability of coal can be marginally improved through the use of an initial pretreatment with supercritical methanol or cyclohexane. Similar treatment with supercritical toluene has the opposite effect. While not presently practical from an economic standpoint, this work may provide new insights into possible avenues for producing alternative fuels from coal. More work needs to be done to determine if the mineral matter liberation can be further improved by varying the conditions and reagents used in the pretreatment.

#### ACKNOWLEDGMENT

The authors would like to thank Robert Kornosky for his assistance in obtaining the gasification chars used in this work and Geno Irdi for performing the microscopic analyses.

#### DISCLAIMER

Reference in this report to any specific product, process, or service is to facilitate understanding and does not necessarily imply its endorsement or favoring by the United States Department of Energy.

#### REFERENCES

1. McCown, F.E., Im, C.J., and Wolfe, R.A., Proceedings of the Second Annual Pittsburgh Coal Conference, 1985, 479.
2. Walters, A.B., ACS Fuel Division Preprints, 29(4), 1984, 337.
3. Kornosky, R.M., Gasior, S.J., Strakey, J.P., and Haynes, W.P., ACS Fuel Division Preprints, 22(2), 1977, 197.
4. Warzinski, R.P., ACS Fuel Division Preprints, 30(3), 1985, 139.

Table 1. Chemical Analysis of Gasification Chars

Coal Type	Subbituminous	Bituminous	Anthracite
Char Yield, wt% of Raw Coal	25	39	45
Proximate Analysis, wt%			
Moisture	1.8	1.3	0.5
Volatile Matter	5.8	1.7	3.1
Fixed Carbon	57.7	72.9	75.6
Ash	34.7	24.2	20.8
Ultimate Analysis, wt% mf			
Carbon	60.3	72.2	74.7
Hydrogen	1.2	1.4	1.1
Nitrogen	0.4	0.7	0.6
Oxygen	3.3	1.4	2.5
Sulfur	0.2	0.3	0.3
Ash	34.7	24.2	20.8
Calorific Value, Btu/lb	9,308	10,622	----

Table 2. Cumulative Washability Results for the Anthracite Coal Gasification Char

Products	--- As-Received ---				--- Crushed ---			
	Yield	Ash	Total Sulfur	Btu/lb	Yield	Ash	Total Sulfur	Btu/lb
	--- wt% mf ---				--- wt% mf ---			
Float 1.60	16.4	3.4	0.45	14,019	3.8	2.2	0.54	14,199
1.60 x 1.80	52.9	6.4	0.41	13,145	4.5	3.4	0.51	13,976
1.80 x 2.00	79.1	7.6	0.33	12,746	44.0	15.9	0.33	11,580
Sink 2.00	100.0	16.7	0.29	11,447	100.0	17.8	0.32	11,259

Table 3. Cumulative Washability Results for the Bituminous Coal Gasification Char

Products	--- As-Received ---				--- Crushed ---			
	Yield	Ash	Total Sulfur	Btu/lb	Yield	Ash	Total Sulfur	Btu/lb
	--- wt% mf ---				--- wt% mf ---			
Float 1.40	63.0	11.2	0.57	12,368	--0--	---	---	-----
1.40 x 1.60	77.2	11.5	0.53	12,265	19.5	3.8	0.80	13,100
1.60 x 1.80	87.0	12.8	0.49	12,103	20.5	4.1	0.78	13,041
1.80 x 1.90	100.0	17.8	0.45	11,354	23.0	5.1	0.73	12,894
1.90 x 2.00	----	----	----	----	98.5	15.7	0.35	10,991
Sink 2.00	----	----	----	----	100.0	17.0	0.35	10,953

Table 4. Cumulative Washability Results for the Subbituminous Coal Gasification Char

Products	--- As-Received ---				--- Crushed ---			
	Yield	Ash	Total Sulfur	Btu/lb	Yield	Ash	Total Sulfur	Btu/lb
	--- wt% mf ---				--- wt% mf ---			
Float 1.60	6.2	7.6	0.38	12,289	5.2	7.2	0.46	12,138
1.60 x 1.80	14.6	8.9	0.23	12,297	5.6	8.8	0.46	11,909
1.80 x 2.20	100.0	32.1	0.19	9,456	97.7	30.0	0.26	8,873
Sink 2.20	----	----	----	-----	100.0	30.1	0.28	8,860

Table 5. Cumulative Washability Results for Illinois No. 6 Coal

Products	Yield	Ash	Total Sulfur	Pyritic Sulfur	Btu/lb
	--- wt% mf ---				
Float 1.25	-0-	----	----	----	-----
1.25 x 1.28	3.4	3.1	2.60	0.45	13,777
1.28 x 1.30	12.8	2.6	2.67	0.37	13,836
1.30 x 1.40	67.5	5.4	3.12	0.78	13,492
1.40 x 1.60	86.4	7.6	3.40	1.14	13,450
Sink 1.60	100.0	13.8	5.02	2.92	12,410
Bulk Sample	-----	14.5	5.10	-----	11,713

Table 6. Cumulative Washability Results for Methanol-Treated Illinois No. 6 Coal

Products	Yield	Ash	Total Sulfur	Pyritic Sulfur	Btu/lb
	--- wt% mf ---				
Float 1.25	-0-	----	----	----	-----
1.25 x 1.28	8.5	1.9	2.50	0.25	13,781
1.28 x 1.30	30.9	2.4	2.59	0.29	13,653
1.30 x 1.40	69.3	5.3	2.86	0.68	13,202
1.40 x 1.60	82.7	7.2	3.14	0.96	12,877
Sink 1.60	100.0	15.3	4.74	2.84	11,485
Bulk Sample	-----	14.9	5.29	-----	11,601

Table 7. Cumulative Washability Results for Cyclohexane-Treated Illinois No. 6 Coal

Products	Yield	Ash	Total Sulfur	Pyritic Sulfur	Btu/lb
	--- wt% mf ---				
Float 1.25	7.4	2.3	2.88	0.41	13,847
1.25 x 1.28	25.5	3.4	2.90	0.19	13,826
1.28 x 1.30	42.7	3.1	3.02	0.16	13,713
1.30 x 1.40	72.7	5.5	3.42	0.17	13,339
1.40 x 1.60	86.4	7.5	3.85	0.18	13,036
Sink 1.60	100.0	14.7	4.38	1.03	12,031
Bulk Sample	-----	15.4	5.38	-----	11,808

**Table 8. Cumulative Washability Results for Toluene-Treated Illinois No. 6 Coal**

Products	Yield	Ash	Total Sulfur	Pyritic Sulfur	Btu/lb
		wt%	mf		
Float 1.25	42.4	8.3	3.22	1.44	12,885
1.25 x 1.28	50.0	8.5	3.24	1.48	12,869
1.28 x 1.30	53.6	8.3	3.21	1.46	12,938
1.30 x 1.40	73.0	8.6	3.22	1.50	12,863
1.40 x 1.60	83.5	9.8	3.41	1.70	12,672
Sink 1.60	100.0	17.3	5.51	3.92	11,465
Bulk Sample	-----	19.3	5.75	-----	11,263

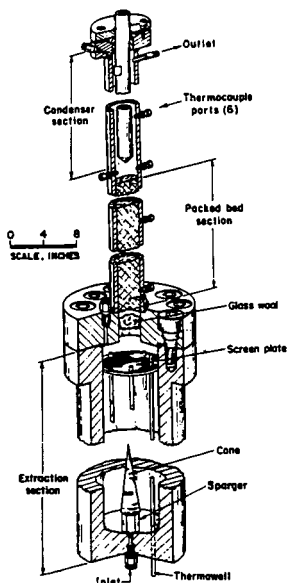


Figure 1. Sectional View of the Supercritical Fluid Extraction Vessel.

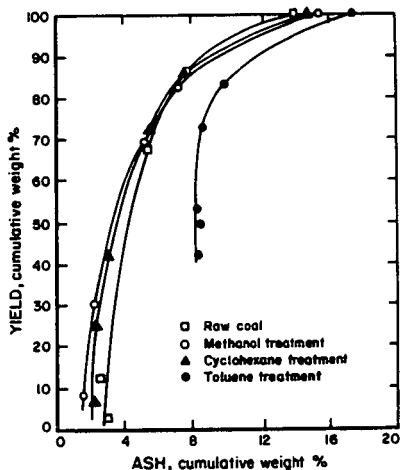


Figure 2. Comparison of Washability Data for Illinois No. 6 Coal Before and After Treatments with Supercritical Methanol, Cyclohexane, and Toluene.

NO. 6880